

## Supplementary information

# Influence of mechanical, thermal, and electrical perturbations on the dielectric behaviour of guest-encapsulated HKUST-1 crystals

Arun Singh Babal and Jin-Chong Tan\*

Multifunctional Materials and Composites (MMC) Laboratory,

Department of Engineering Science, University of Oxford,

Parks Road, Oxford, OX1 3PJ, U.K.

\* [jin-chong.tan@eng.ox.ac.uk](mailto:jin-chong.tan@eng.ox.ac.uk)

## Contents

1. Morphological and topological studies on HKUST-1 MOF powder and pellets .....	3
1.1 Particle size measurement .....	3
1.1.1 Scanning electron microscopy (SEM) .....	3
1.1.2 Atomic force microscopy (AFM) .....	4
2. Fourier transform Infrared spectroscopy (FTIR) of pressure pellets .....	5
3. Effect of pelleting pressure on FWHM (Full width at half maximum) value of the characteristic XRD peak	6
4. N <sub>2</sub> Adsorption-desorption and thermal stability of HKUST-1 samples .....	9
5. Optical microscopy for pellet roughness measurements .....	10
5.1 HKUST-1-S pellets .....	10
5.2 HKUST-1-T pellets .....	12
6. Dielectric properties of activated HKUST-1 .....	14
6.1 Real part of dielectric constant ( $\epsilon'$ ) .....	14
6.1.1 HKUST-1-S pellets .....	14
6.1.2 HKUST-1-T pellets .....	16
6.2 Imaginary part of dielectric constant ( $\epsilon''$ ) .....	18
6.2.1 HKUST-1-S pellets .....	18
6.2.2 HKUST-1-T pellets .....	20
6.3 Loss tangent ( $\tan \delta$ ) .....	22
6.3.1 HKUST-1-S pellets .....	22
6.3.2 HKUST-1-T pellets .....	24
7. Dielectric properties under ambient conditions (44% RH) .....	26
7.1 Real part of dielectric constant ( $\epsilon'$ ) .....	26

7.2	Imaginary part of dielectric constant ( $\epsilon''$ ) .....	27
7.3	Loss Tangent ( $\tan \delta$ ) .....	28
8	Conductivity measurements .....	29
8.1	AC conductivity ( $\sigma_{AC}$ ) .....	29
8.1.1	HKUST-1-S pellets .....	29
8.1.2	HKUST-1-T pellets .....	31
8.2	Impedance measurements ( $Z^*$ ) .....	33
8.2.1	HKUST-1-S pellets .....	33
8.2.3	Complex impedance of pellets at ambient conditions (44% RH) .....	37
9	Equivalent circuit data fitting of impedance plot .....	38
9.1	HKUST-1-S pellets .....	38
9.2	HKUST-1-T .....	40

# 1. Morphological and topological studies on HKUST-1 MOF powder and pellets

## 1.1 Particle size measurement

### 1.1.1 Scanning electron microscopy (SEM)

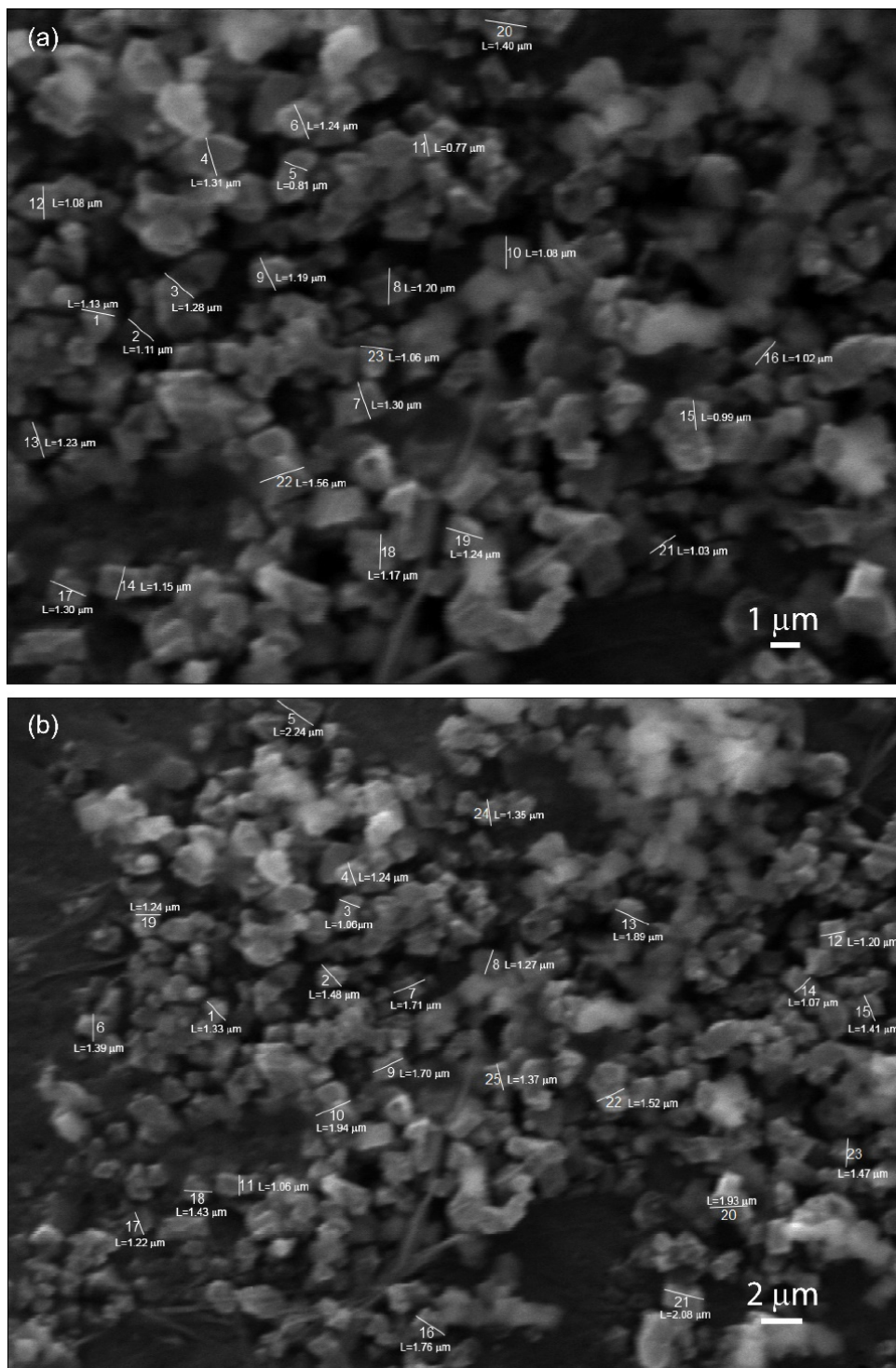


Figure S1: Measurement of total 50 individual particles of HKUST-1-S from the SEM images. The averaged particle size is  $1.5 \pm 0.74 \mu\text{m}$ .

### 1.1.2 Atomic force microscopy (AFM)

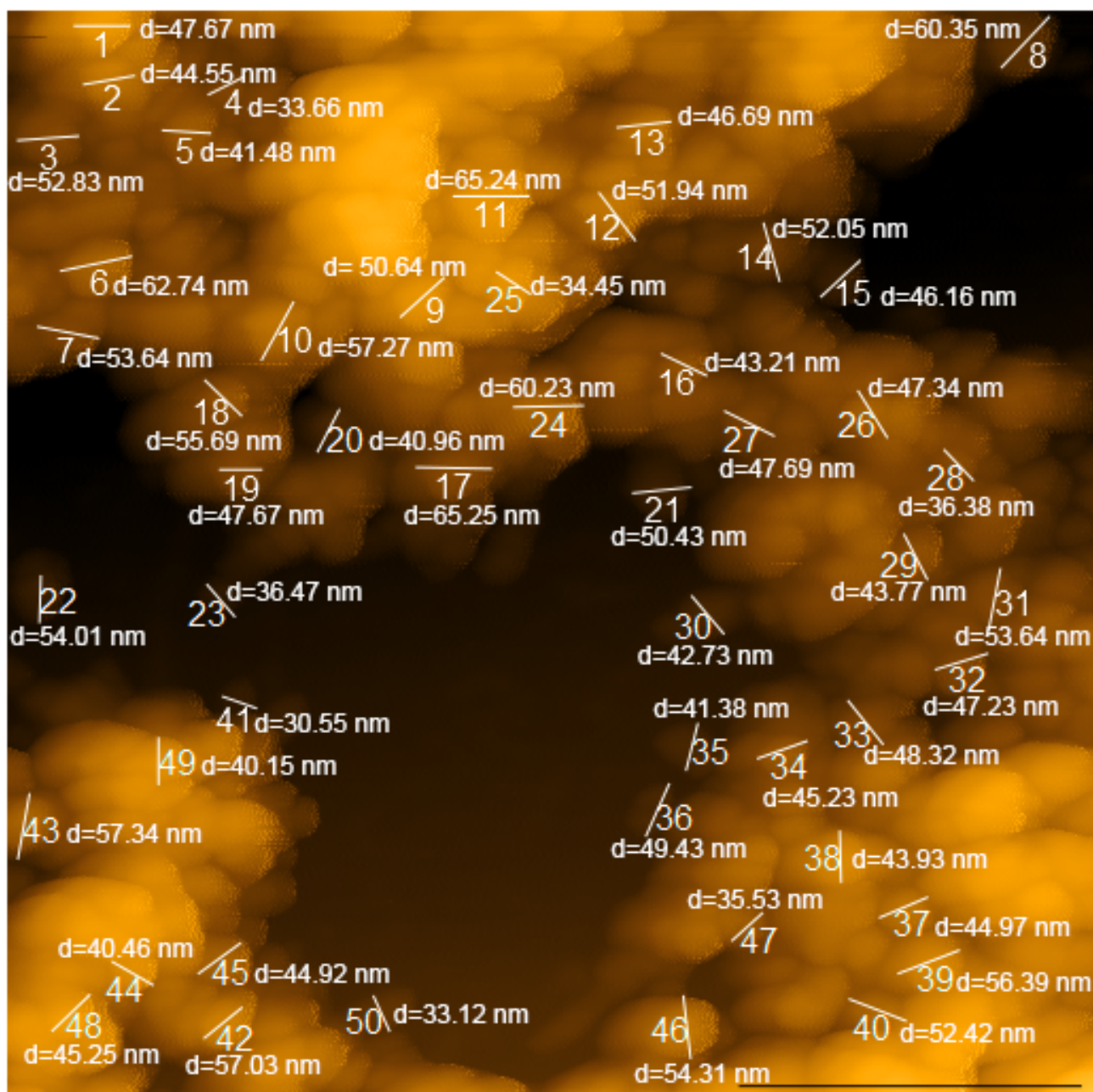


Figure S2: Measurement of total 50 individual particles of HKUST-1-S from the AFM image. The averaged particle size is  $47.89 \pm 17.36$  nm.

## 2. Fourier transform Infrared spectroscopy (FTIR) of pressure pellets

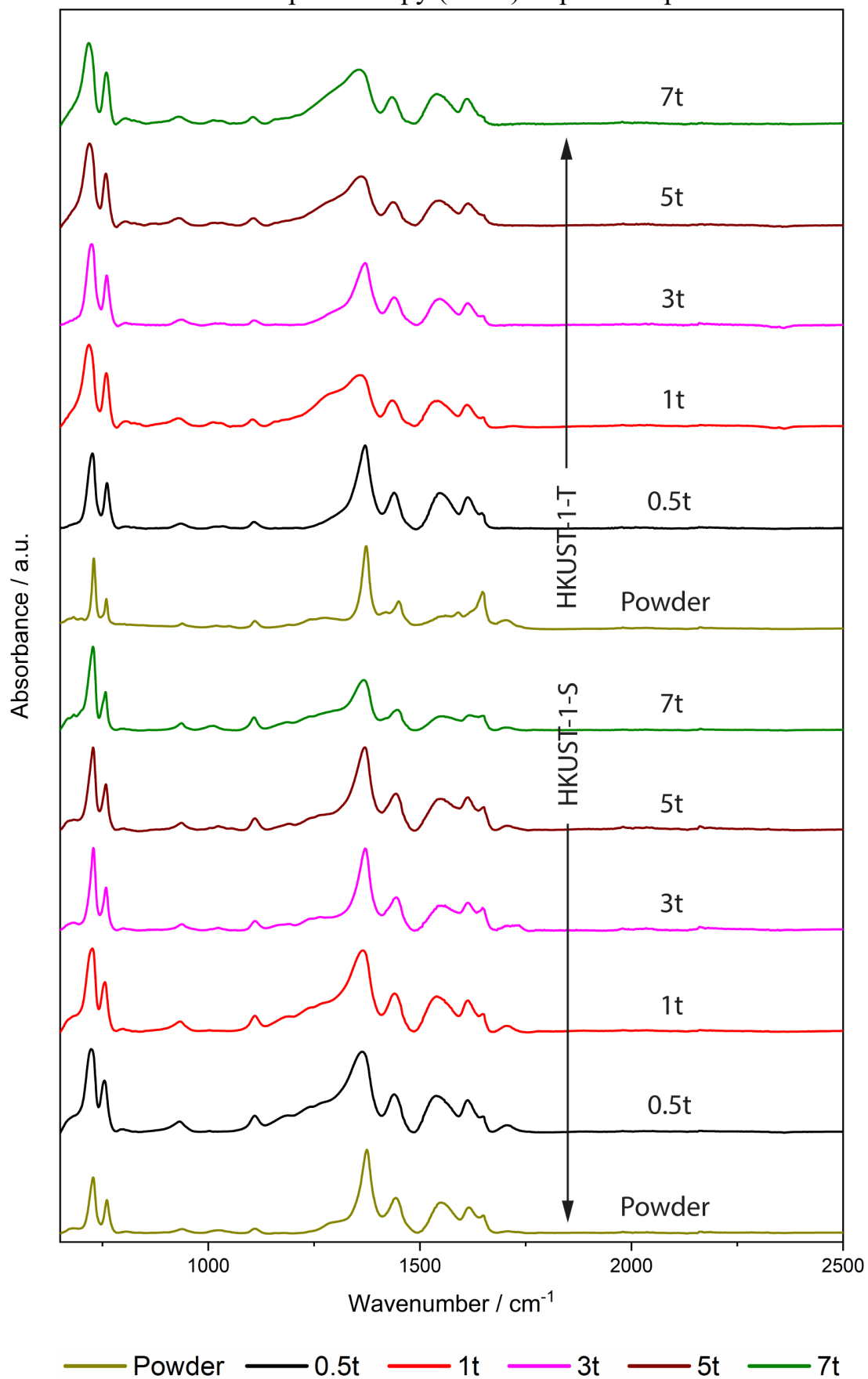
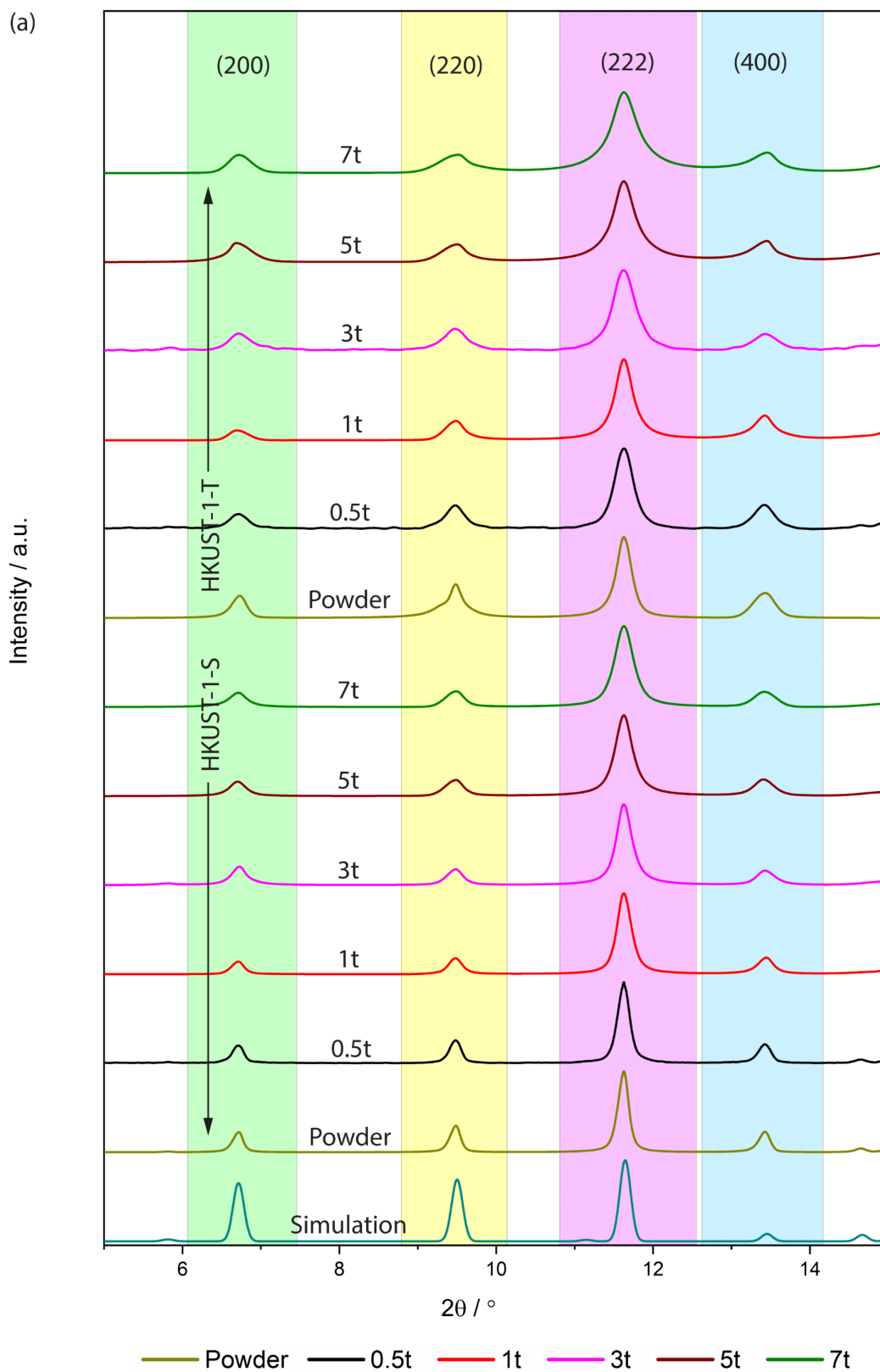


Figure S3: Normalized FTIR spectra of different type of HKUST-1-S and HKUST-1-T MOF pressure pellets.

### 3. Effect of pelleting pressure on FWHM (Full width at half maximum) value of the characteristic XRD peak



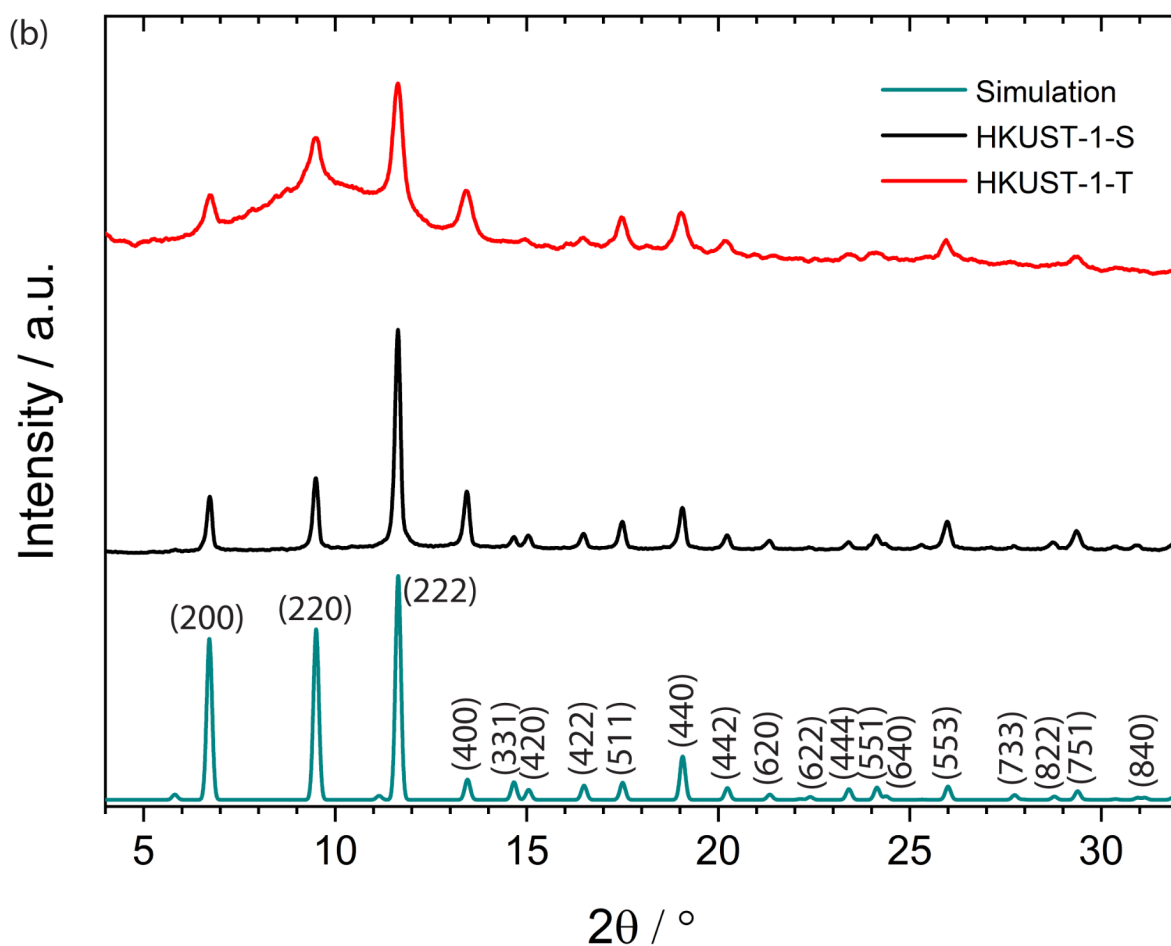


Figure S4: (a) XRD patterns of the HKUST-1 pellets prepared under a compressive force of 0.5t to 7t. (b) Comparison of the simulated XRD pattern of HKUST-1 with the as-synthesized powders of HKUST-1-S and HKUST-1-T (both without background subtraction), normalized to the (222) peak which has the highest intensity. HKUST-1-T exhibits a broad peak from  $2\theta$  of  $\sim 6^\circ$  to  $14^\circ$  that superimpose the sharp Bragg peaks in the same region, thereby suggesting the presence of some semi-crystalline or amorphous products.

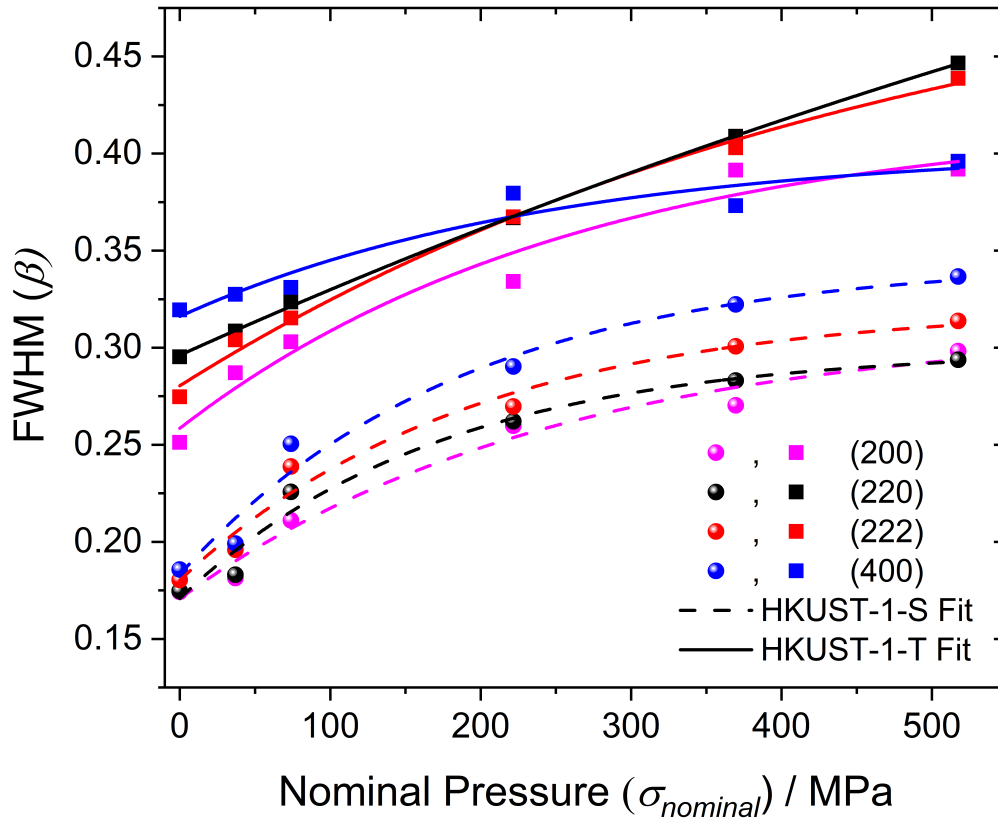


Figure S5: FWHM vs pelleting pressure plot for HKUST-1-S and HKUST-1-T samples.

#### 4. N<sub>2</sub> Adsorption-desorption and thermal stability of HKUST-1 samples

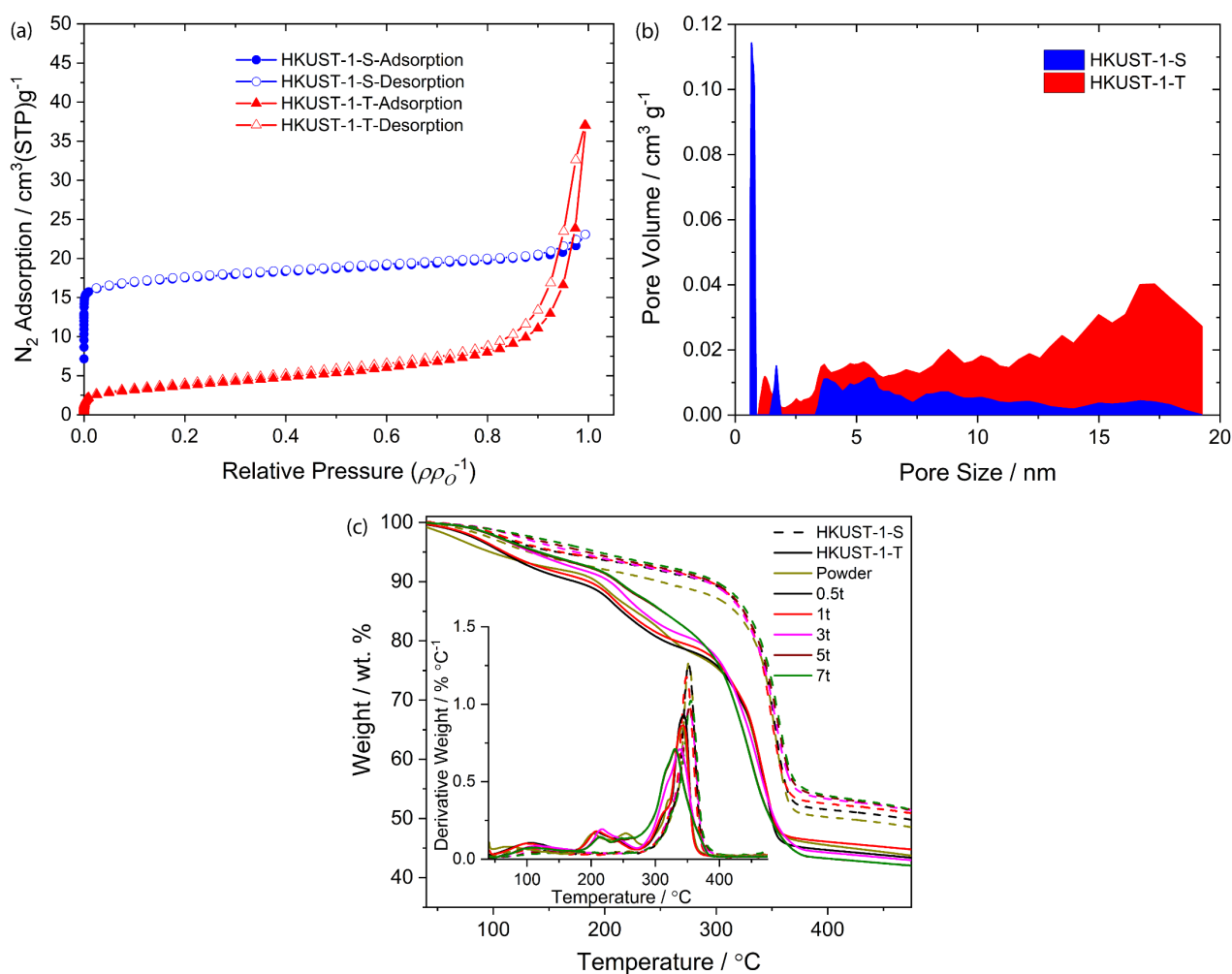
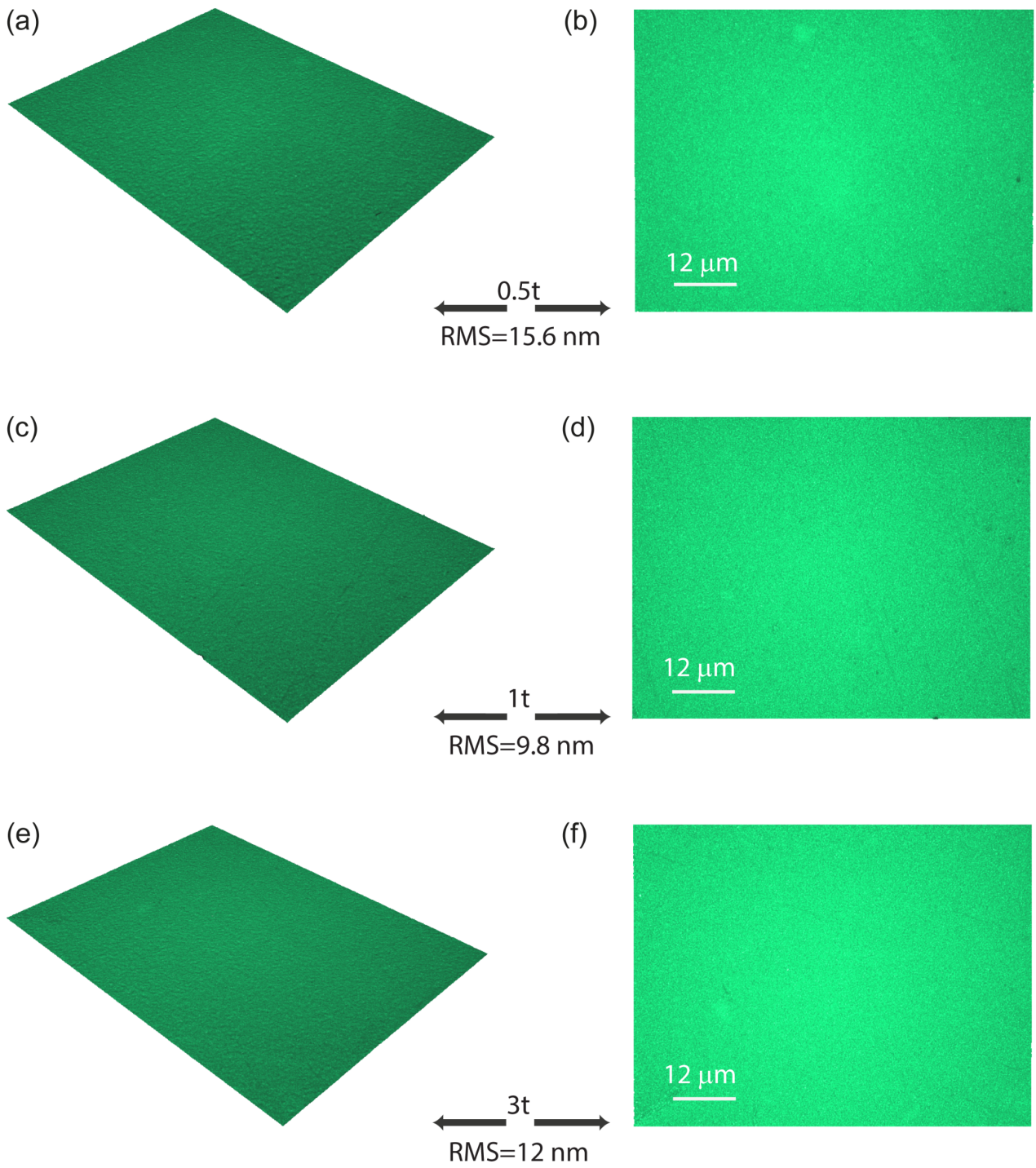


Figure S6: (a) Nitrogen adsorption-desorption isotherms of powder samples of HKUST-1-S (blue) and HKUST-1-T (red) at 77 K. The BET surface areas of the HKUST-1-S and HKUST-1-T samples are 1007 m<sup>2</sup>/g and 165 m<sup>2</sup>/g, respectively. (b) Pore size distributions determined from non-linear DFT model, assuming a combination of slit-shape and cylindrical-shape pores typically applied in MOF analysis. HKUST-1-S has predominantly micropores of <math> < 2\text{ nm}</math>, whereas HKUST-1-T is comprising mesopores from *ca.* 2-20 nm. (c) Thermo-gravimetric analysis plot of HKUST-1 samples as a function of temperature. The hump in the derivative plot suggests the presence of NEt<sub>3</sub> molecules resulted in [Cu<sub>3</sub>(BTC)<sub>2</sub>].1.5N(CH<sub>2</sub>CH<sub>3</sub>)<sub>3</sub>.

## 5. Optical microscopy for pellet roughness measurements

### 5.1 HKUST-1-S pellets



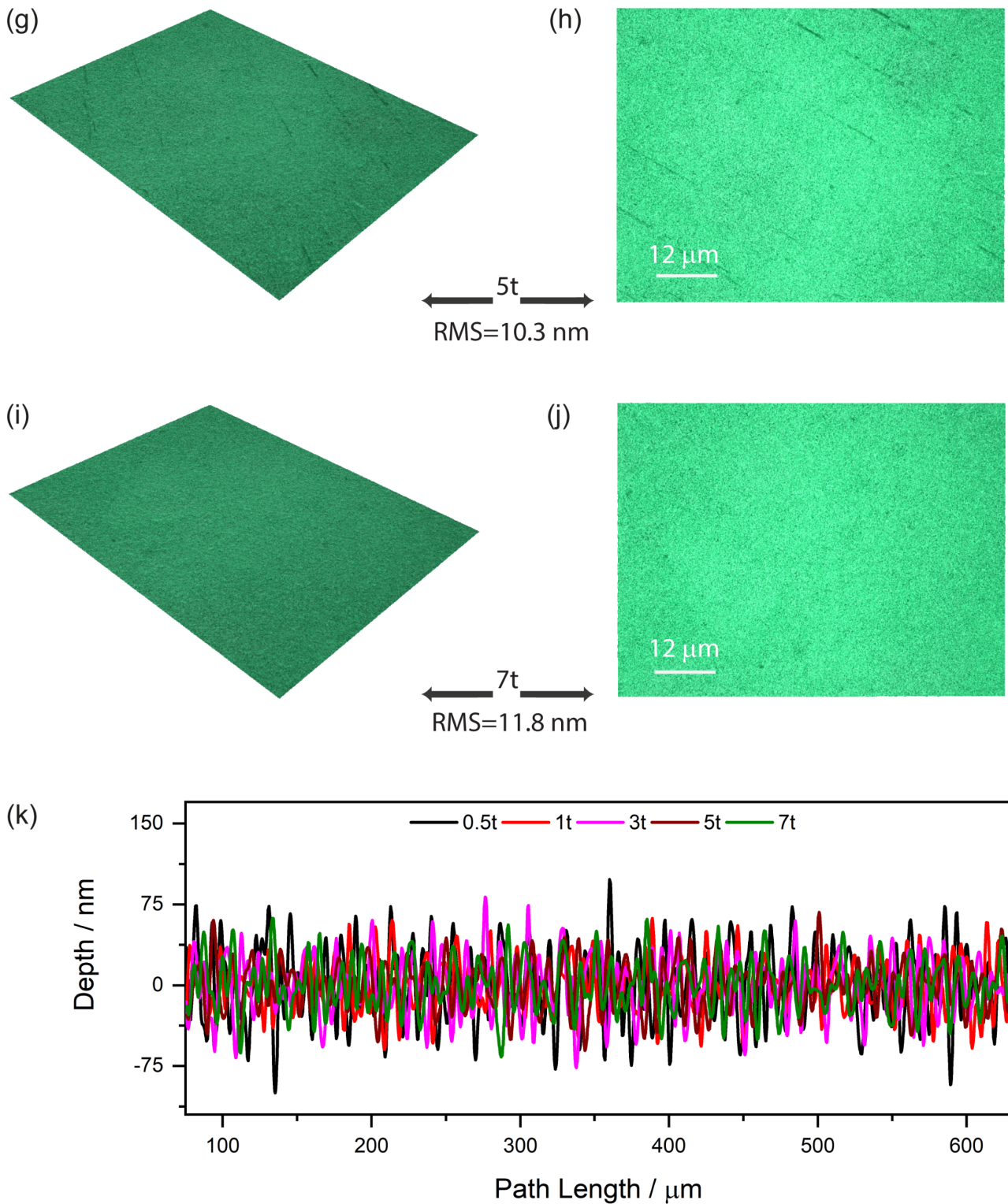
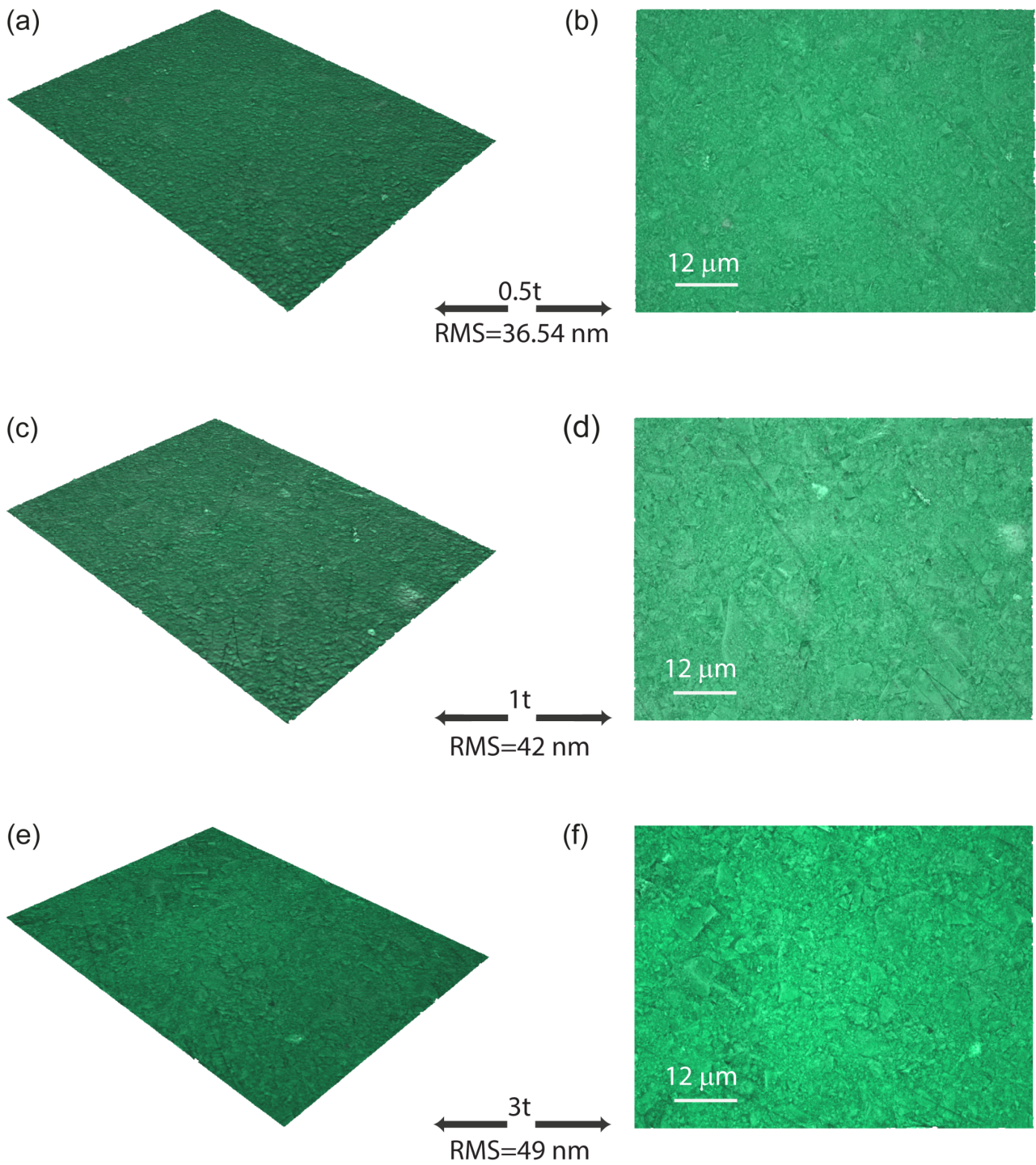


Figure S7: HKUST-1-S pellet surface roughness characterization using Alicona Infinite Focus Microscope at 20× optical magnification: (a)-(b) 0.5 ton, (c)-(d) 1 ton, (e)-(f) 3 ton, (g)-(h) 5 ton, (i)-(j) 7 ton, (k) pellet roughness profile by using the profile line width of 80 μm, respectively. (RMS=Root mean square roughness of profile)

## 5.2 HKUST-1-T pellets



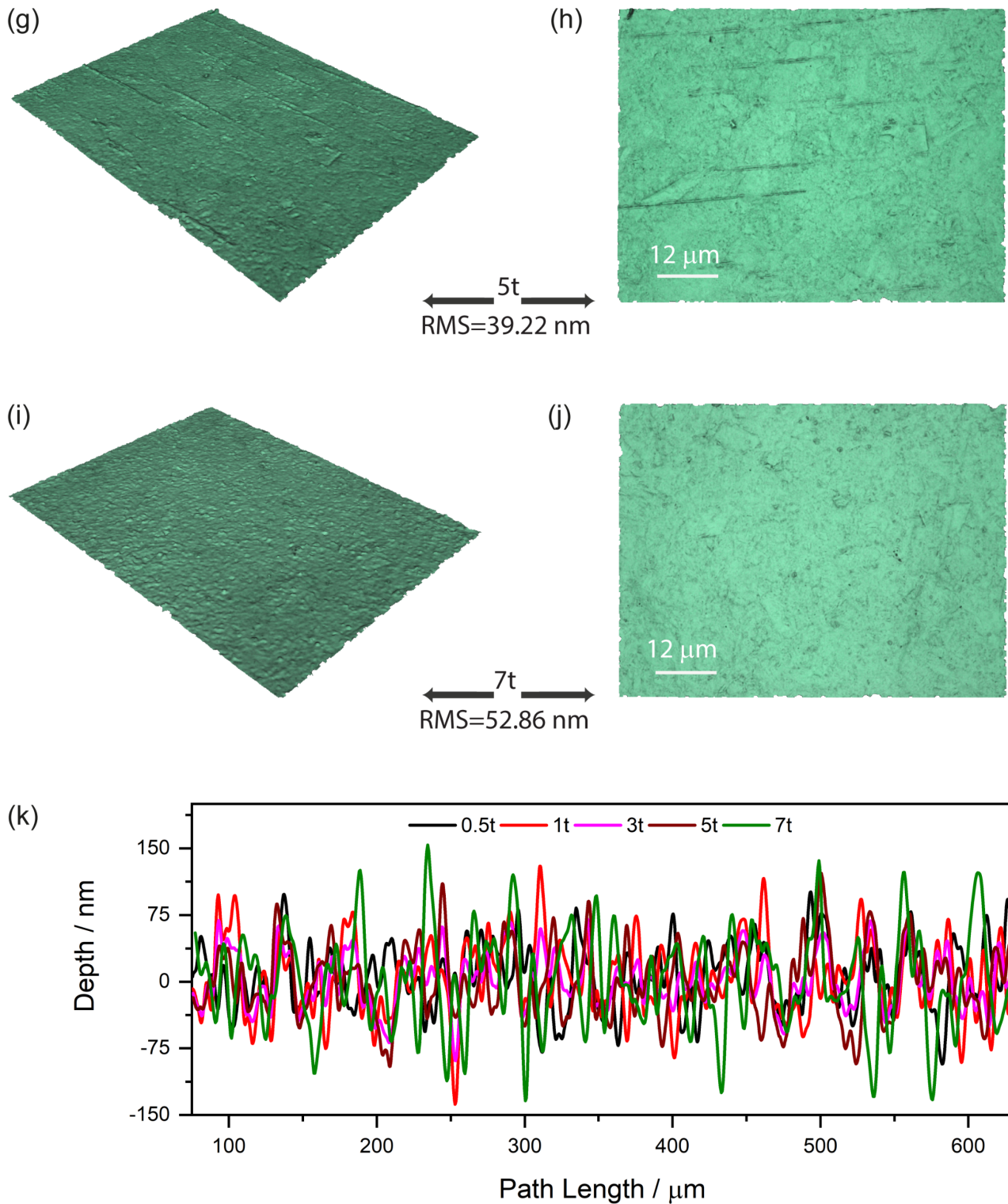
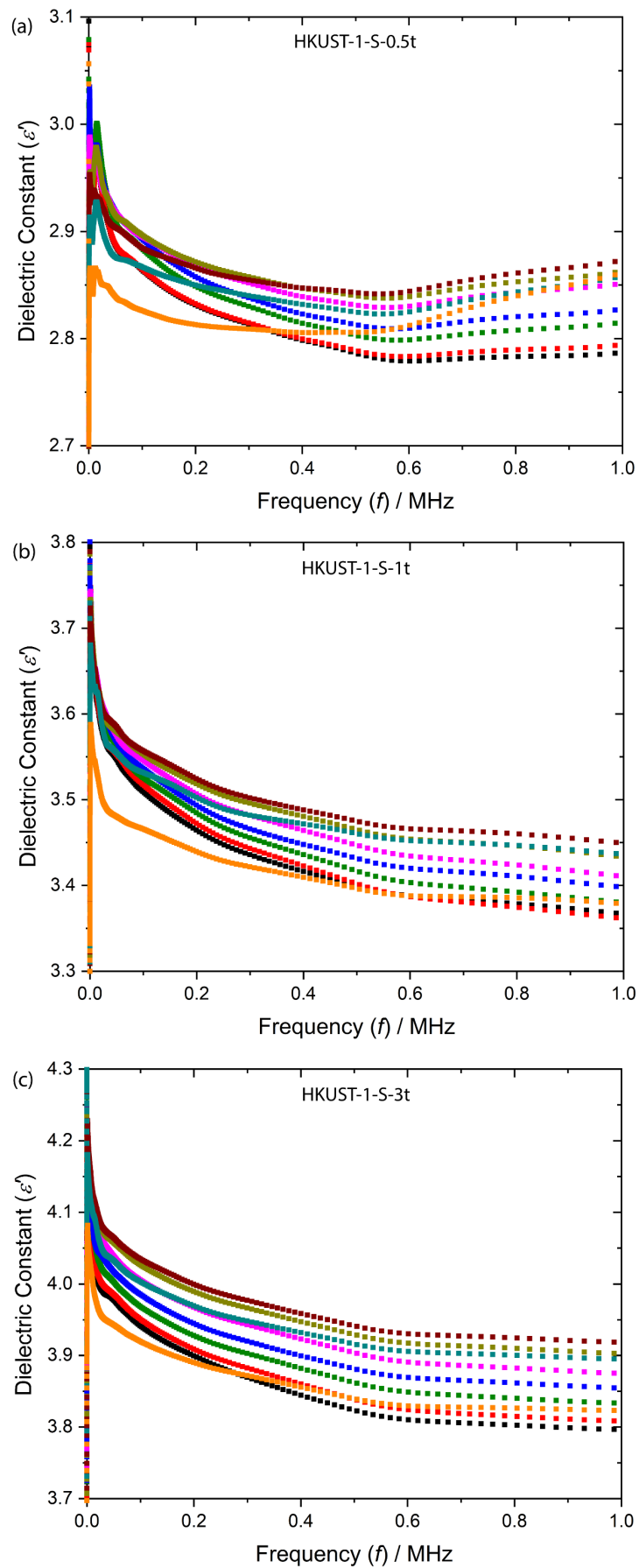


Figure S8: HKUST-1-T pellet surface roughness characterization using Alicona Infinite Focus Microscope at 20× optical magnification: (a)-(b) 0.5 ton, (c)-(d) 1 ton, (e)-(f) 3 ton, (g)-(h) 5 ton, (i)-(j) 7 ton, (k) pellet roughness profile by using the profile line width of 80 μm, respectively. (RMS=Root mean square roughness of profile)

## 6. Dielectric properties of activated HKUST-1

### 6.1 Real part of dielectric constant ( $\epsilon'$ )

#### 6.1.1 HKUST-1-S pellets



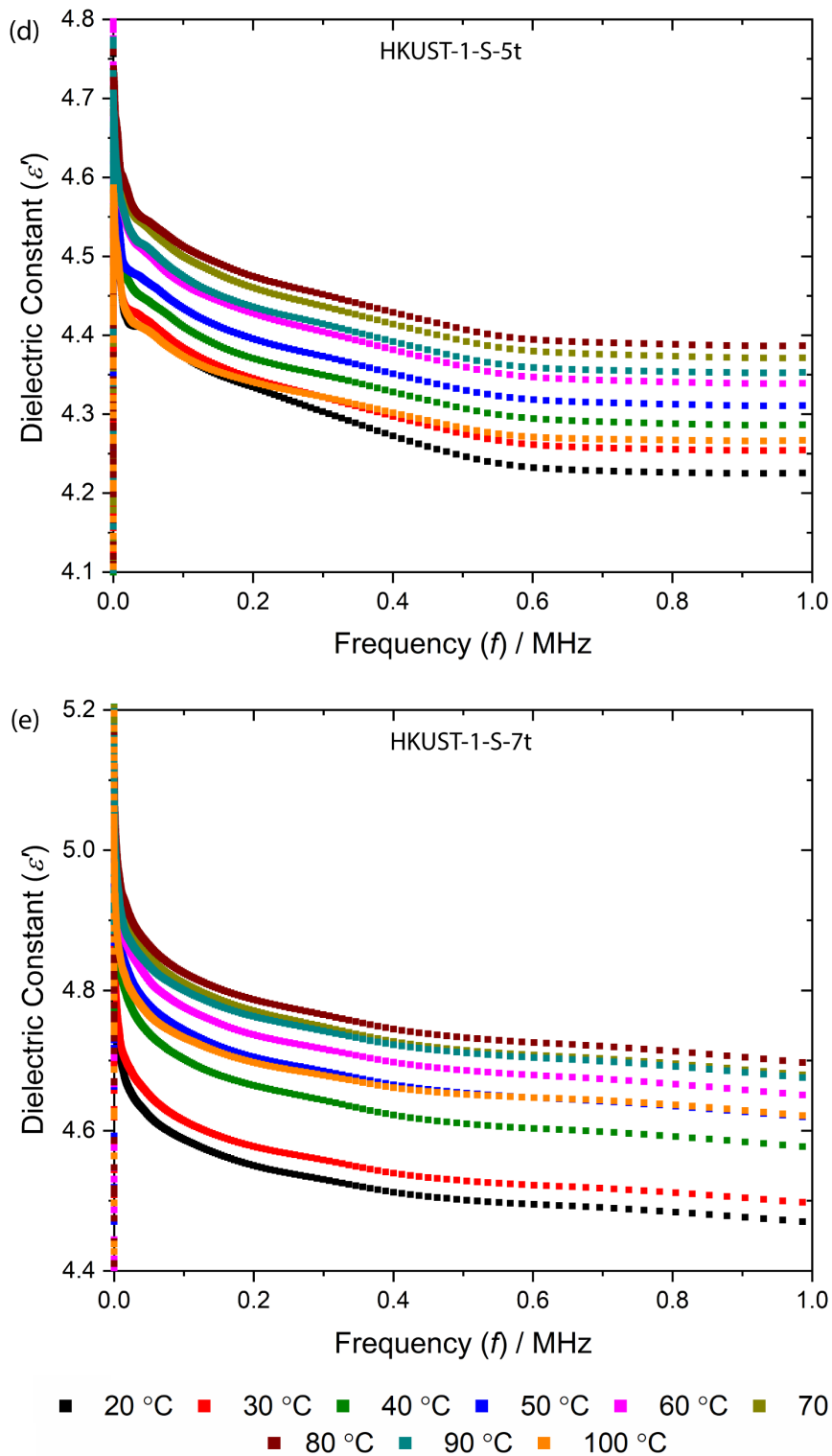
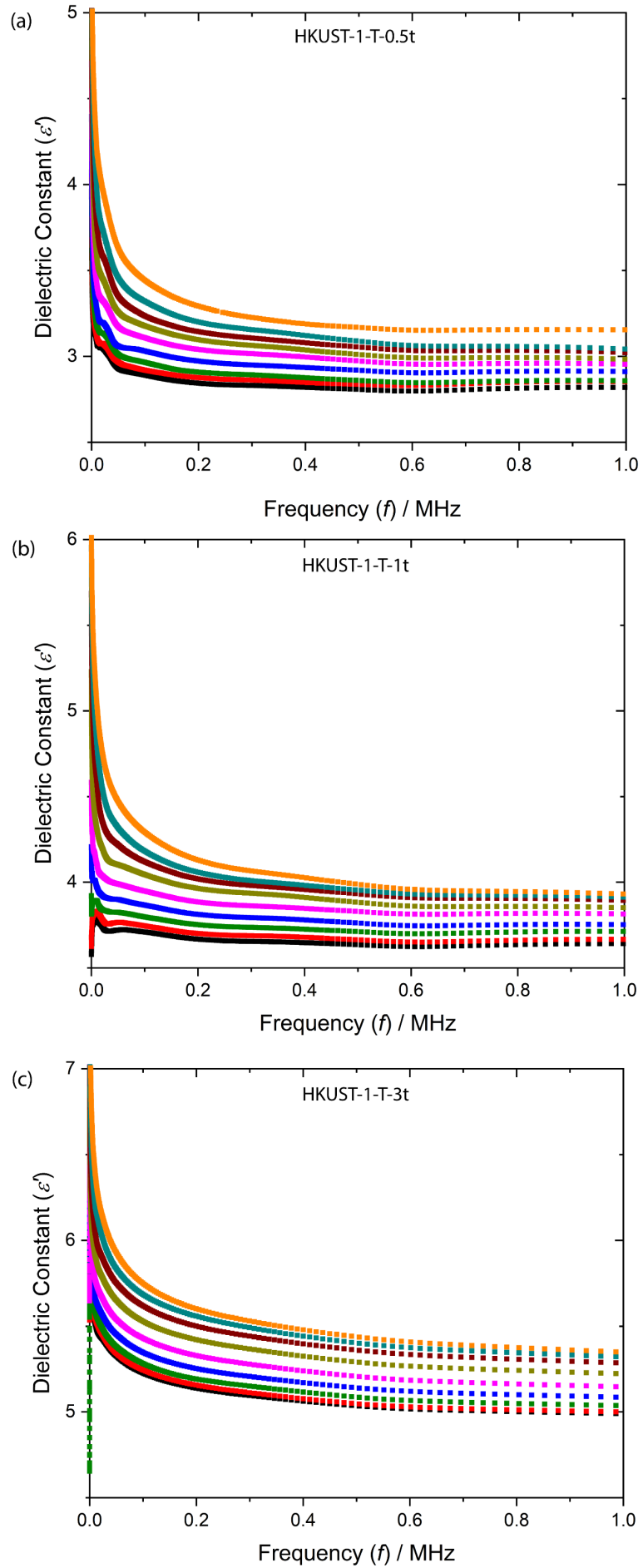


Figure S9: Temperature dependent real part of the dielectric constant as a function of frequency for HKUST-1-S pellets prepared under a compression load of: (a) 0.5 ton, (b) 1 ton, (c) 3 ton, (d) 5 ton and (e) 7 ton, corresponding to the pressure of 36.96, 73.92, 221.76, 369.6 and 517.44 MPa, respectively

### 6.1.2 HKUST-1-T pellets



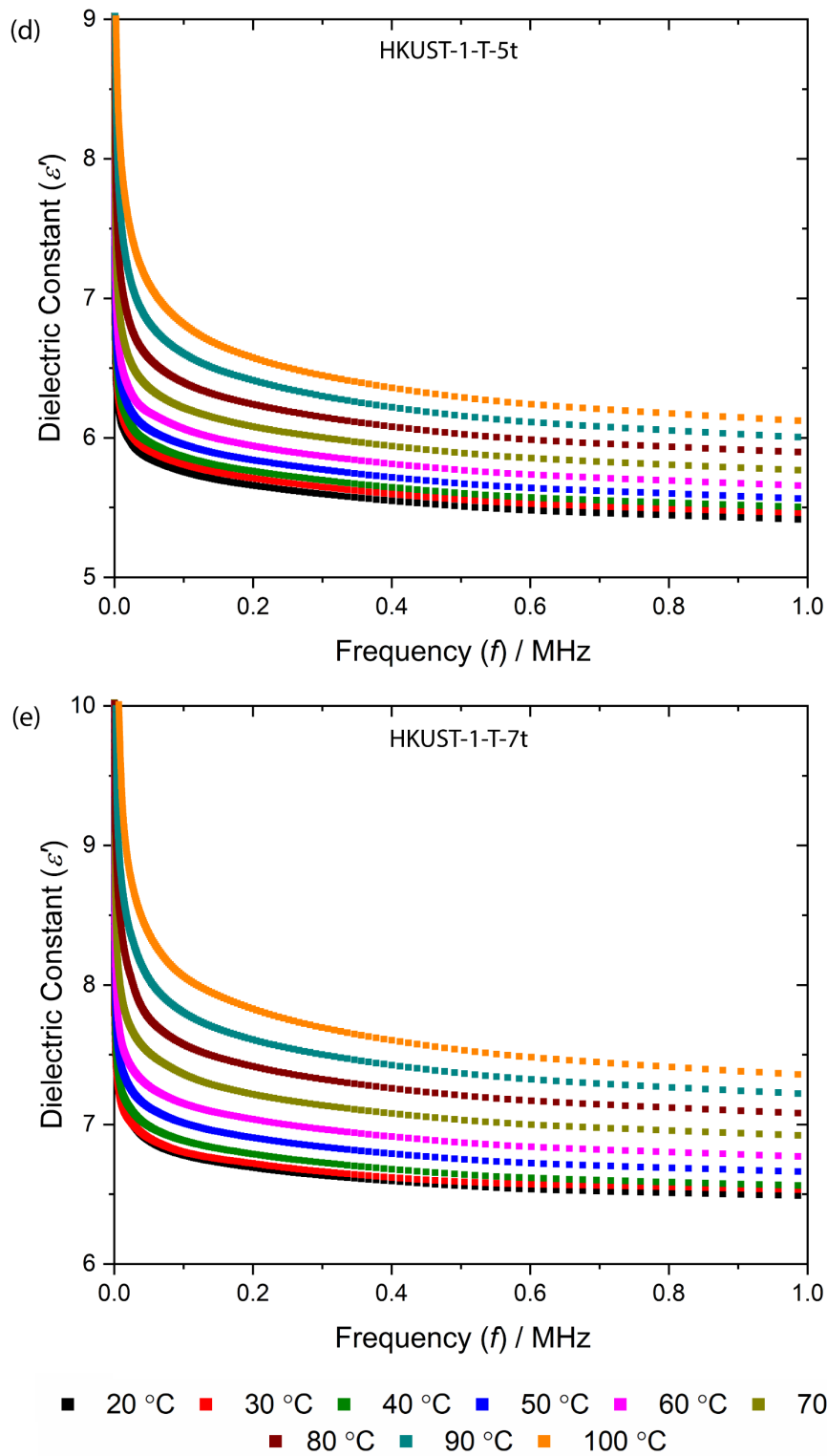
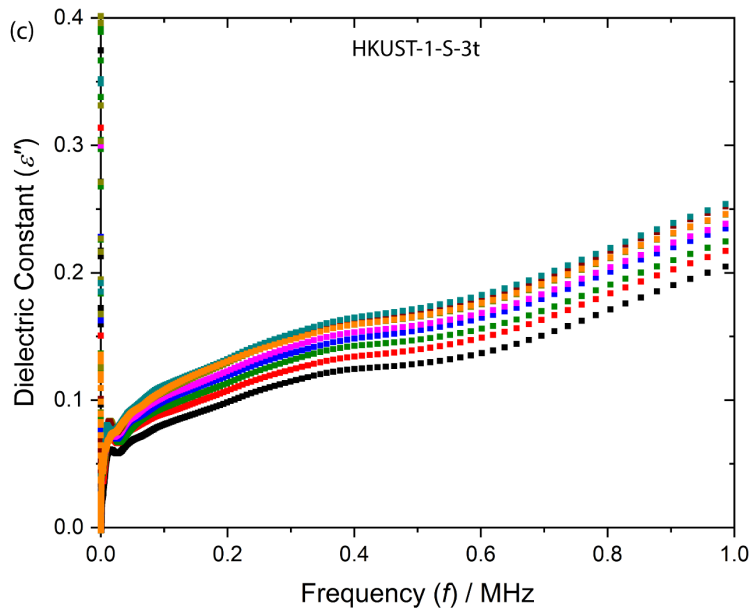
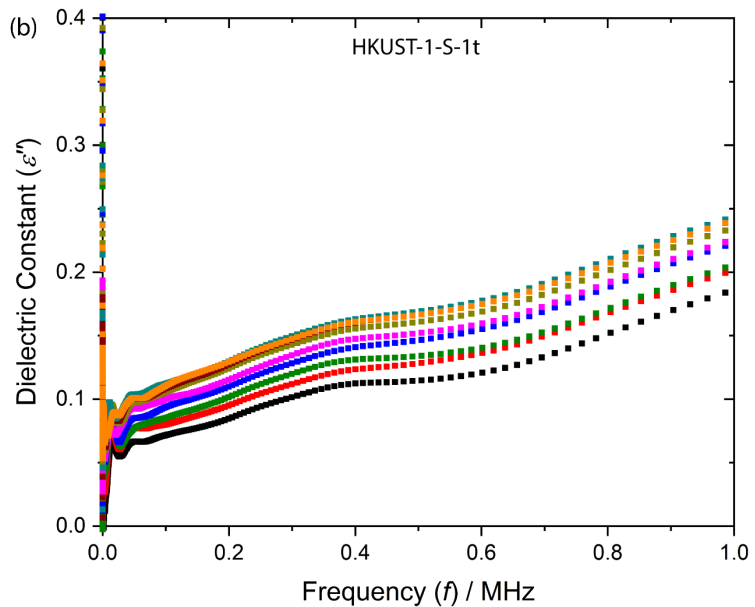
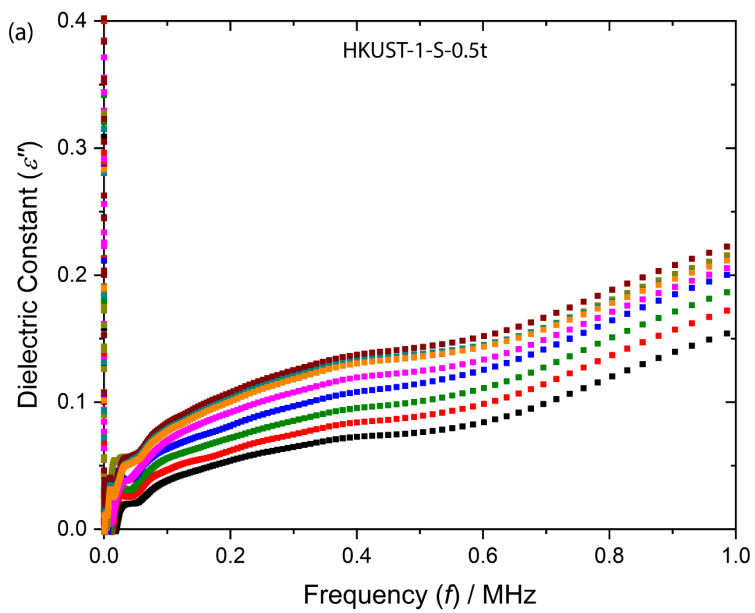


Figure S10: Temperature dependent real part of dielectric constant as a function of frequency for HKUST-1-T pellets: (a) 0.5 ton, (b) 1 ton, (c) 3 ton, (d) 5 ton and (e) 7 ton.

## 6.2 Imaginary part of dielectric constant ( $\epsilon''$ )

### 6.2.1 HKUST-1-S pellets



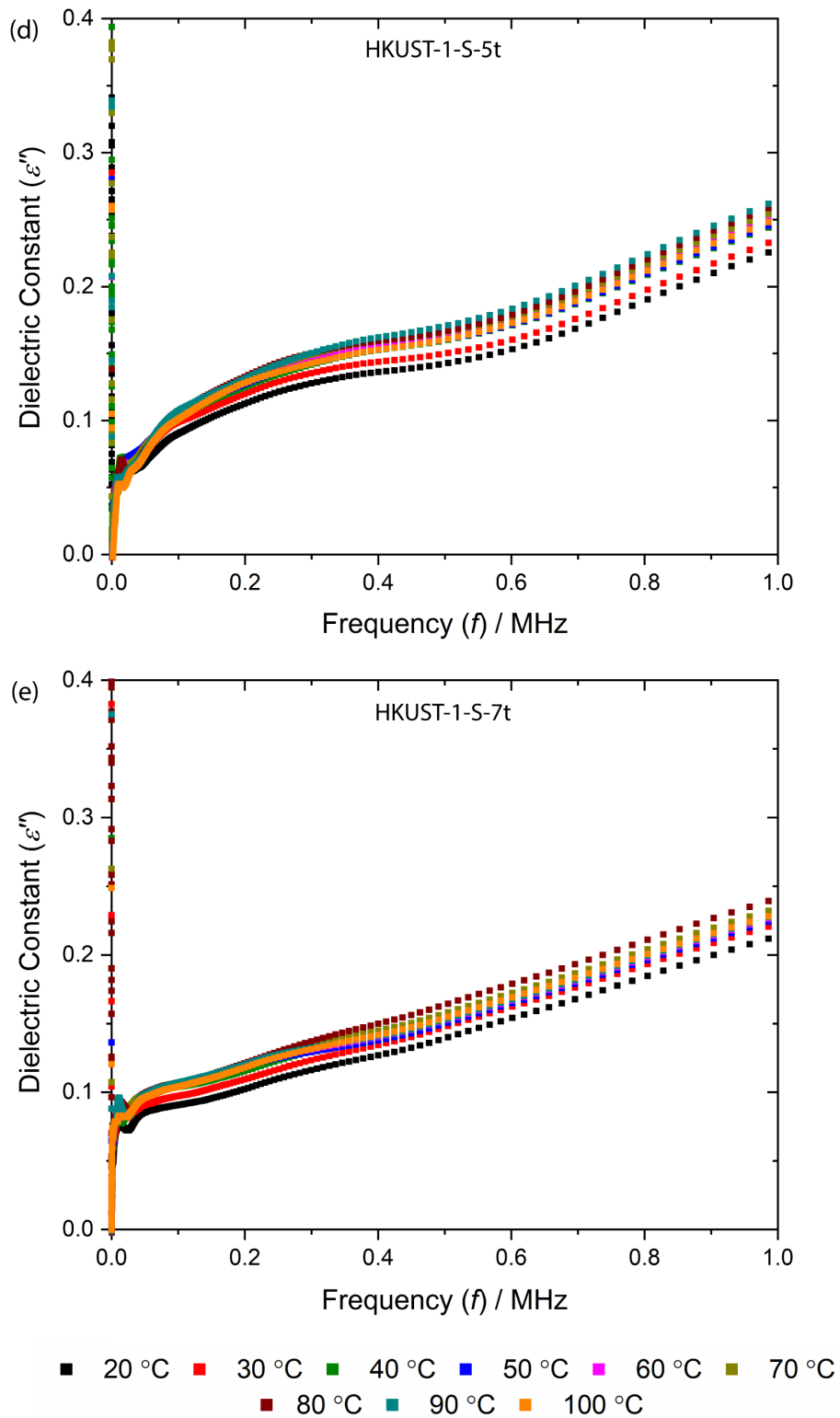
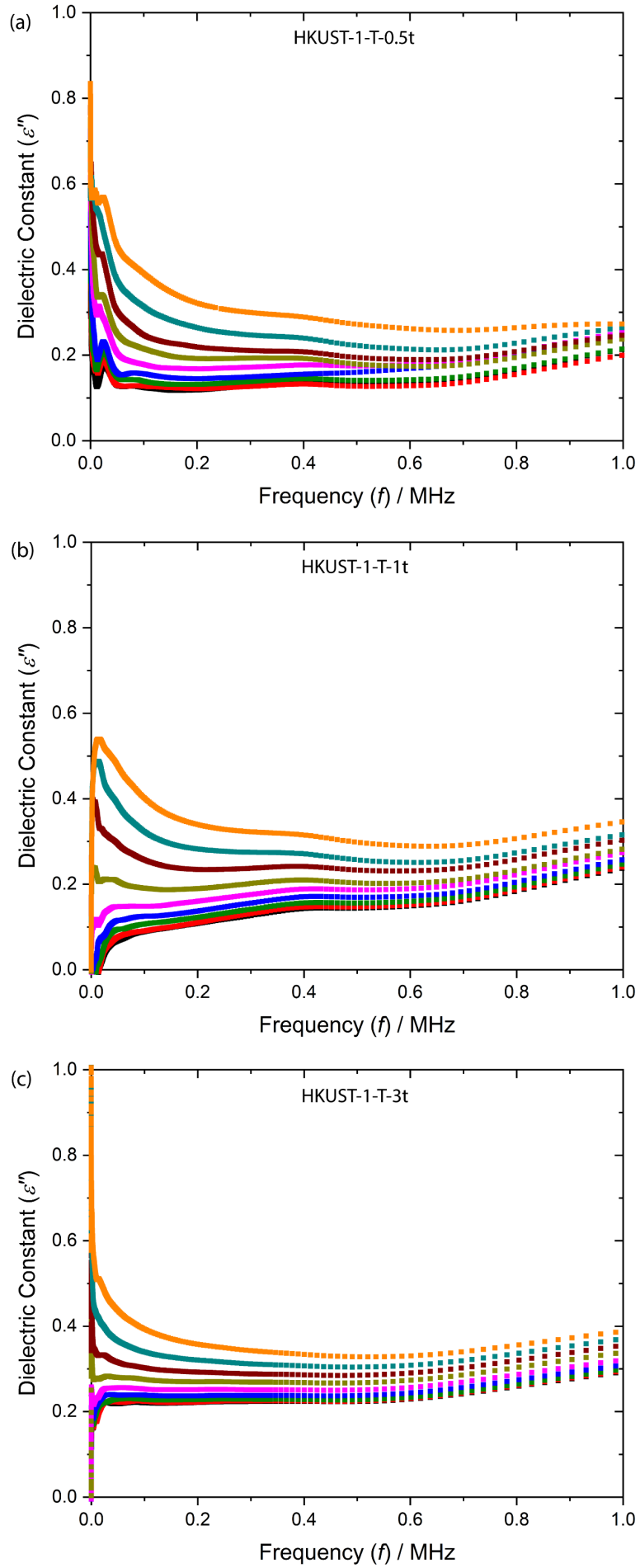


Figure S11: Temperature dependent imaginary part of the dielectric constant as a function of frequency for HKUST-1-S pellets prepared under a compression load of: (a) 0.5 ton, (b) 1 ton, (c) 3 ton, (d) 5 ton and (e) 7 ton, corresponding to the pressure of 36.96, 73.92, 221.76, 369.6 and 517.44 MPa, respectively.

## 6.2.2 HKUST-1-T pellets



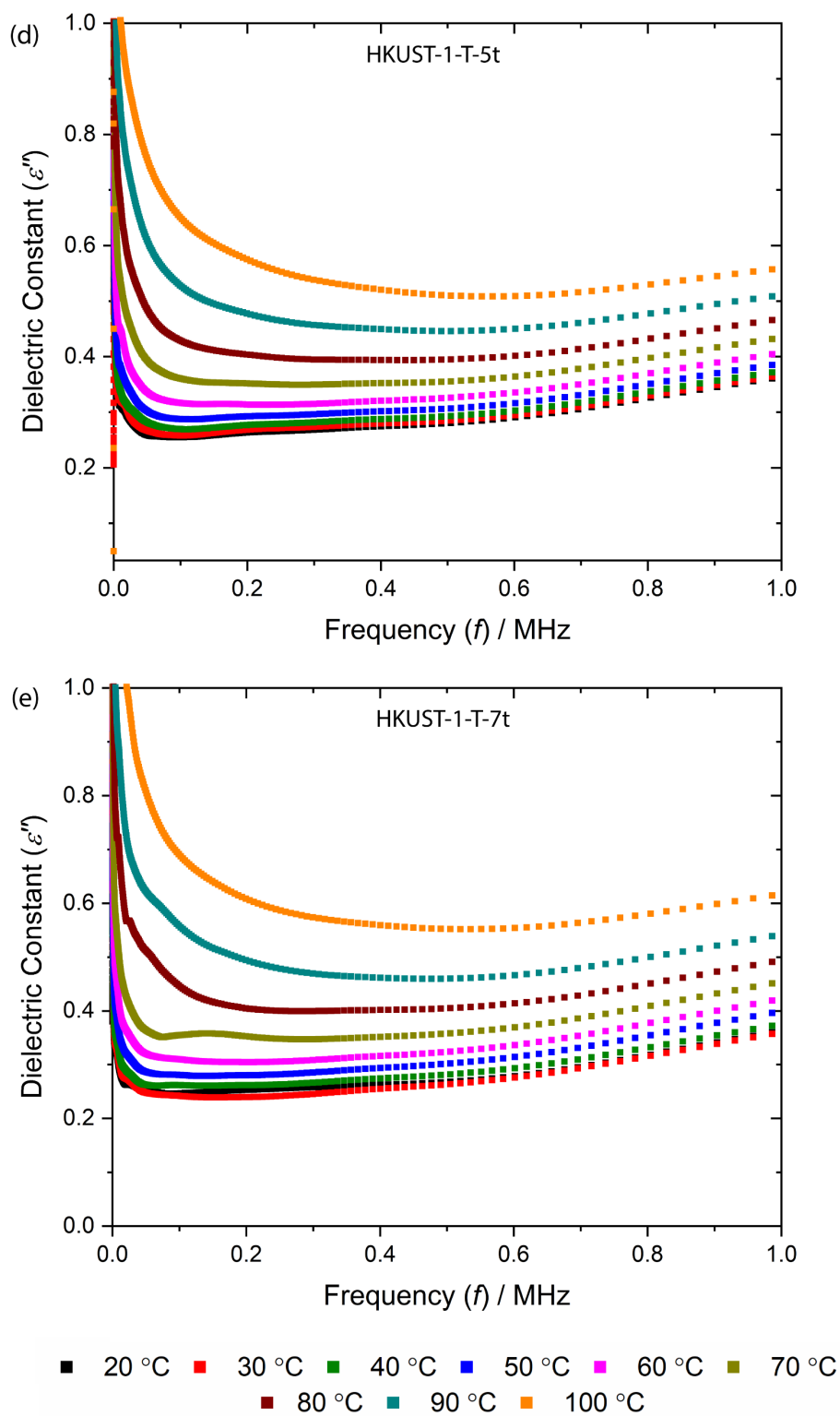
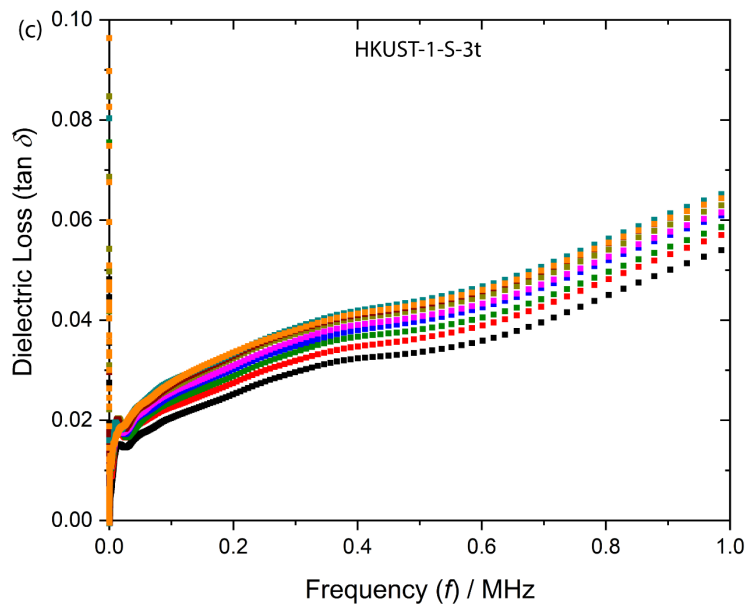
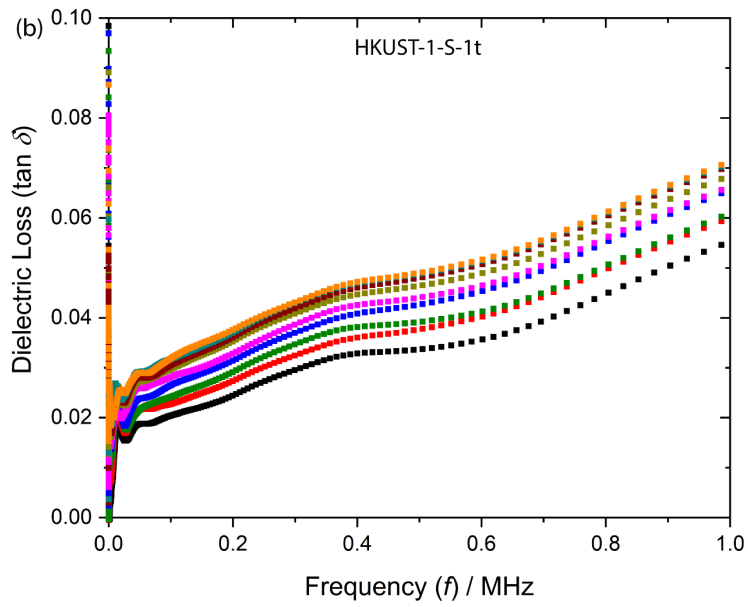
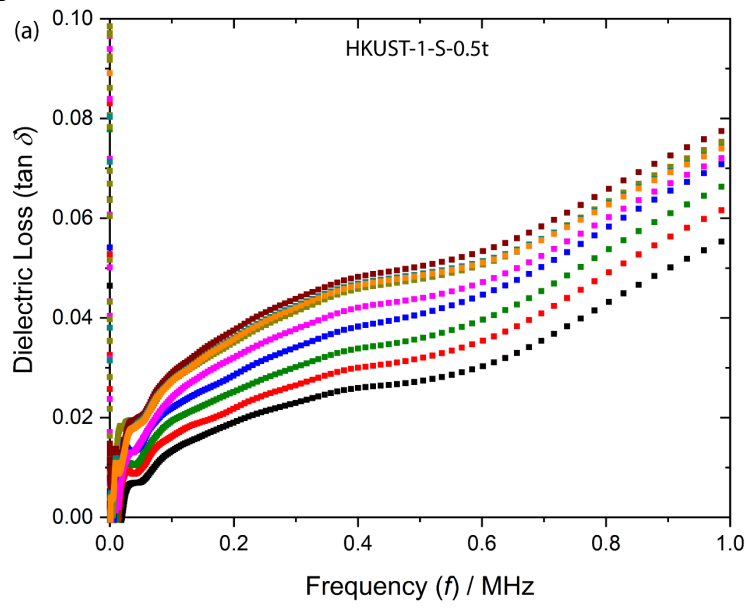


Figure S12: Temperature dependent Imaginary part of dielectric constant as a function of frequency for HKUST-1-T pellets: (a) 0.5 ton, (b) 1 ton, (c) 3 ton, (d) 5 ton and (e) 7 ton.

### 6.3 Loss tangent ( $\tan \delta$ )

#### 6.3.1 HKUST-1-S pellets



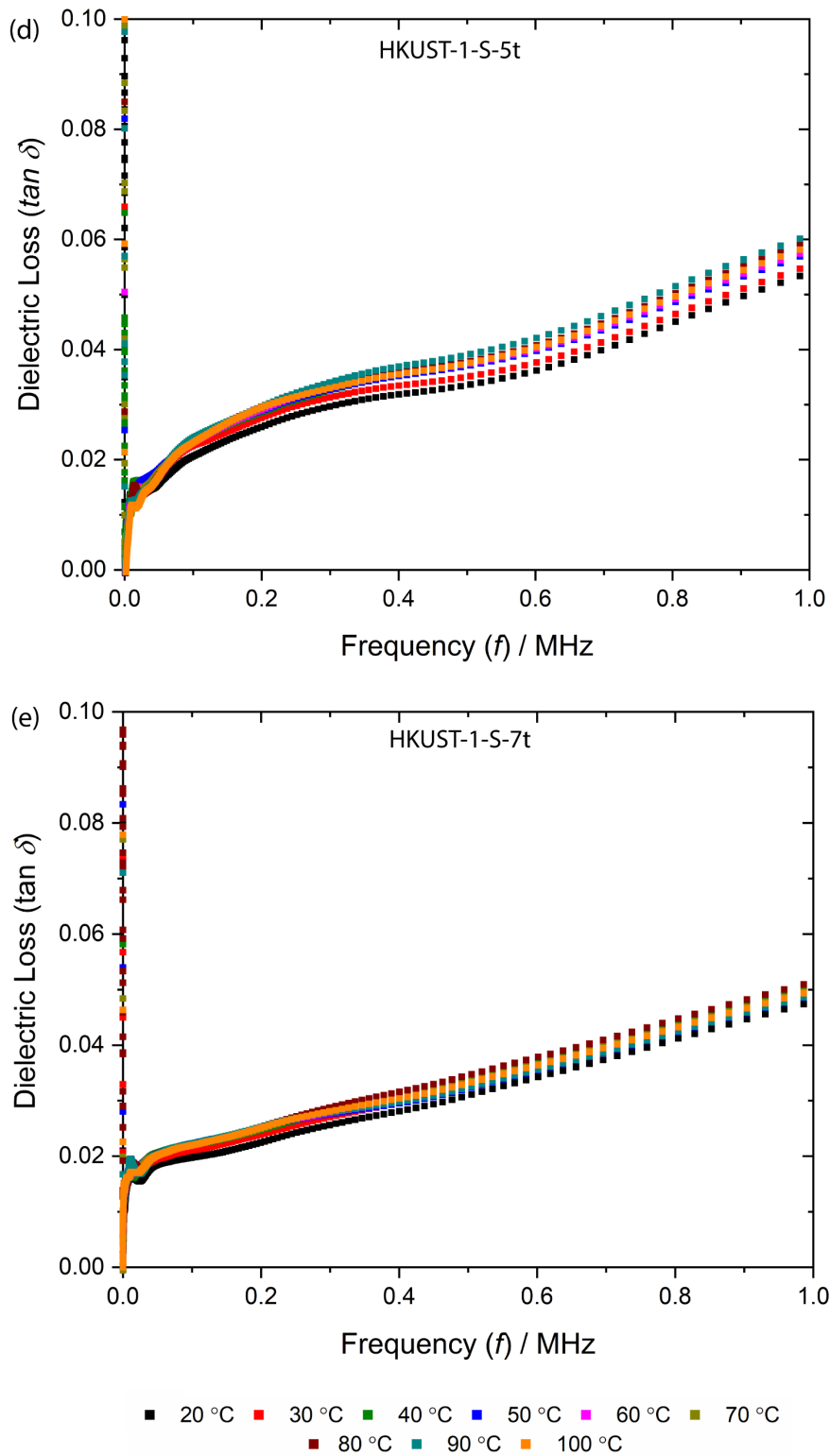
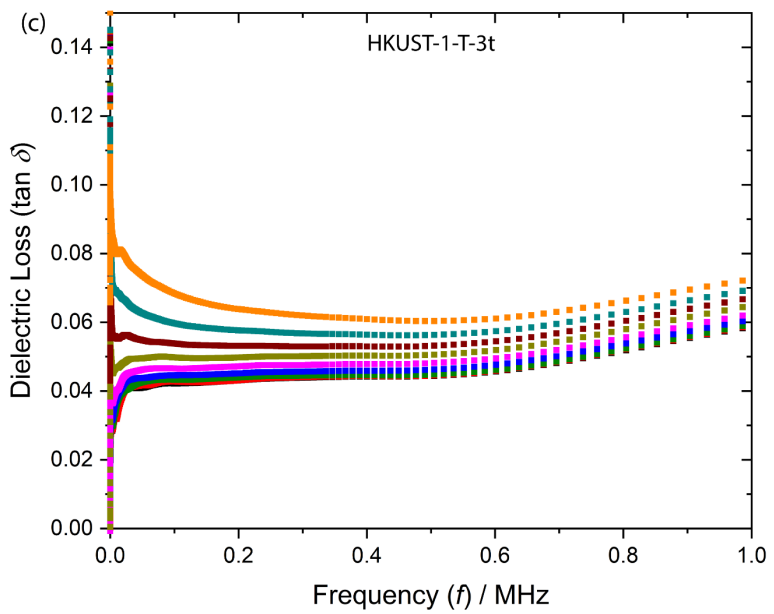
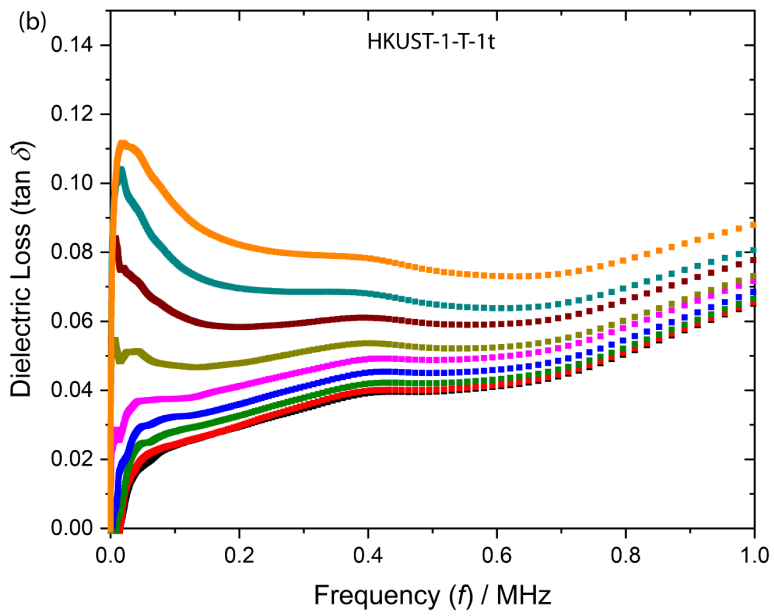
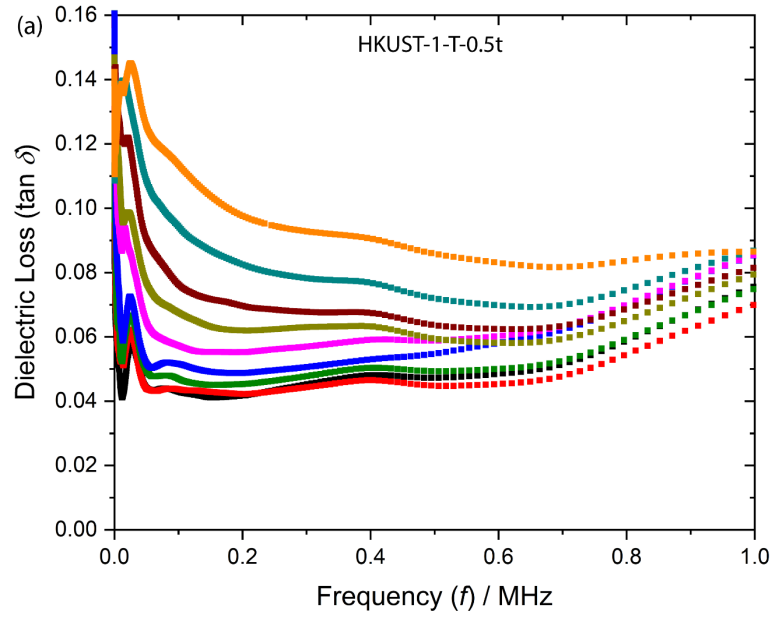


Figure S13: Temperature dependent dielectric loss as a function of frequency for HKUST-1-S pellets prepared under a compression load of: (a) 0.5 ton, (b) 1 ton, (c) 3 ton, (d) 5 ton and (e) 7 ton, corresponding to the pressure of 36.96, 73.92, 221.76, 369.6 and 517.44 MPa, respectively.

### 6.3.2 HKUST-1-T pellets



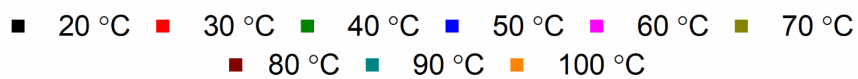
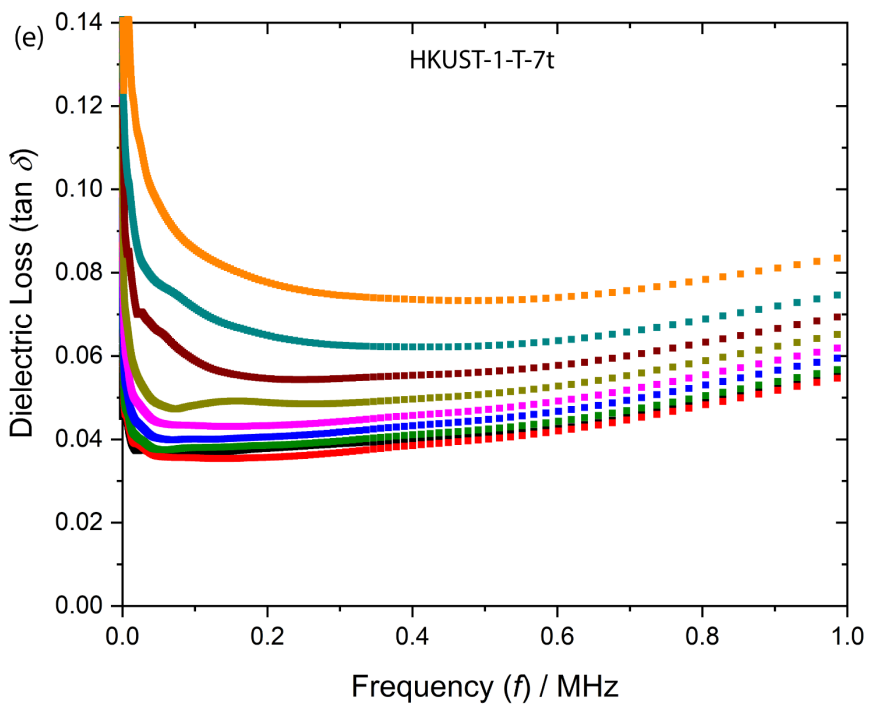
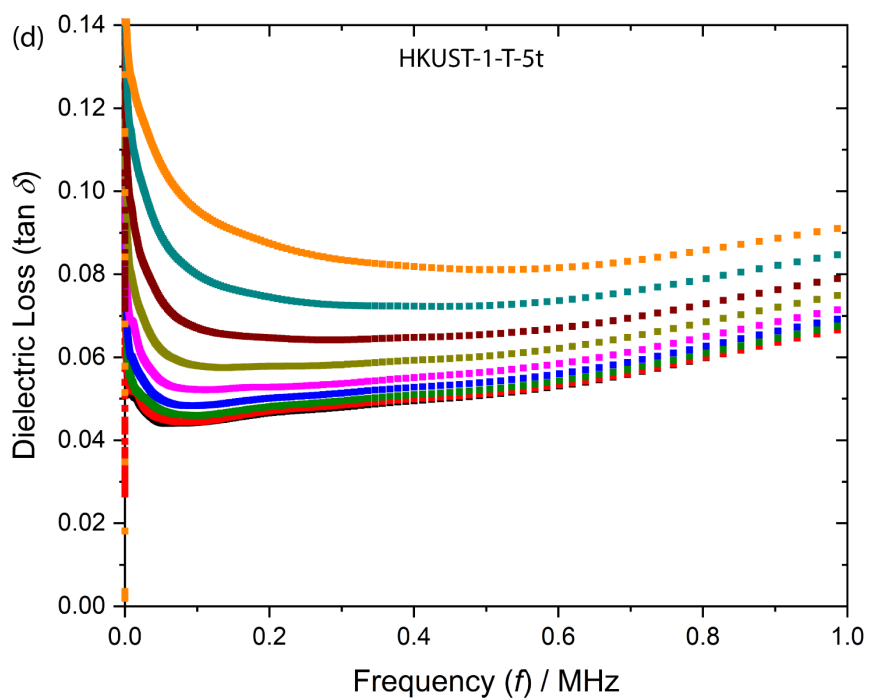


Figure S14: Temperature dependent dielectric loss as a function of frequency for HKUST-1-T pellets: (a) 0.5 ton, (b) 1 ton, (c) 3 ton, (d) 5 ton and (e) 7 ton.

## 7 Dielectric properties under ambient conditions (44% RH)

### 7.1 Real part of dielectric constant ( $\epsilon'$ )

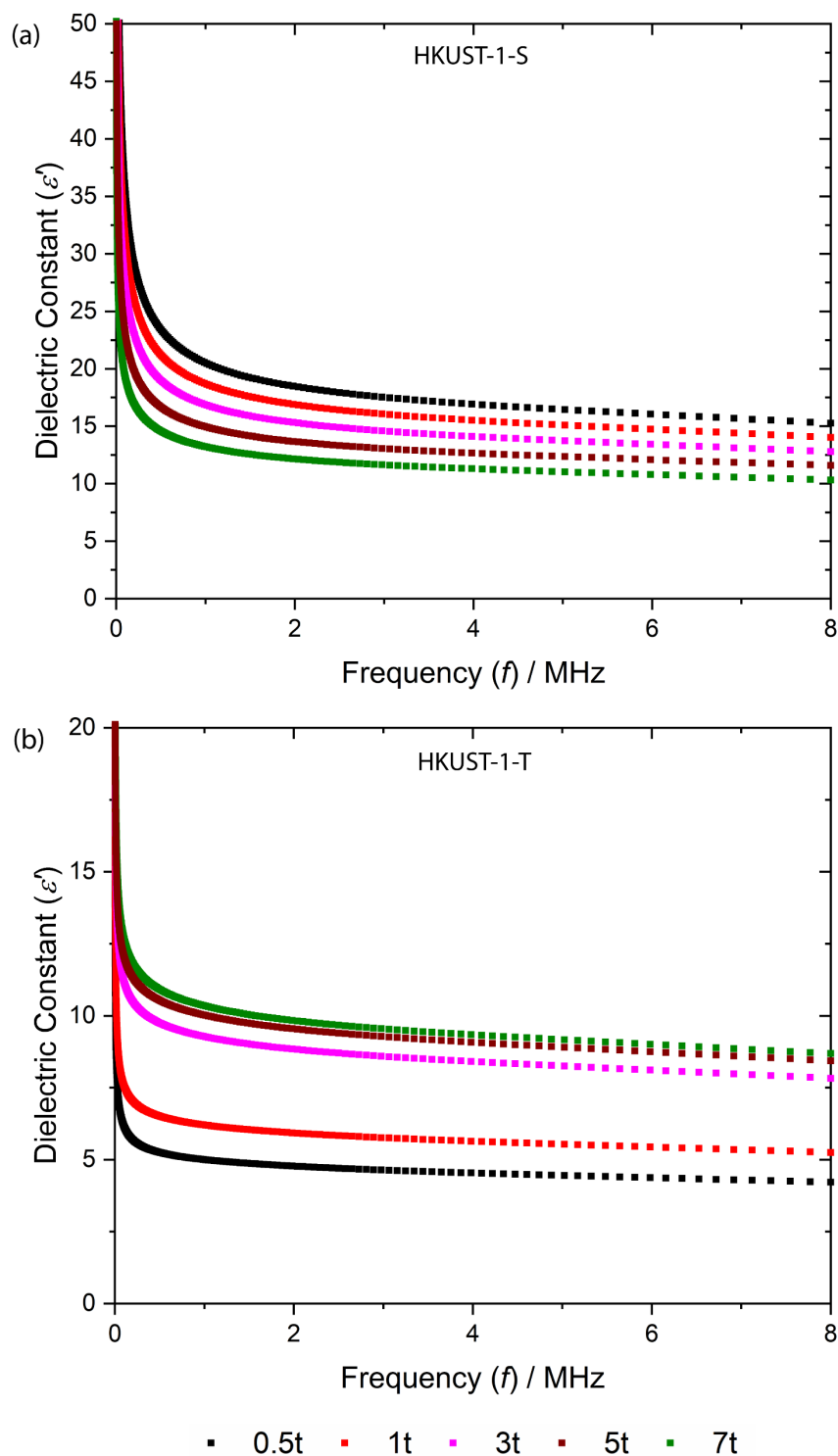


Figure S15: Real part of dielectric constant of (a) HKUST-1-S and (b) HKUST-1-T pellets at ambient condition (44% RH). The HKUST-1-T pellets shows relatively lower  $\epsilon'$  value over HKUST-1-S pellets due to the presence of  $\text{NEt}_3$  molecule in the pore causing lesser moisture adsorption. In the case of HKUST-1-T samples, the  $\epsilon'$  value increases with pelleting pressure up to a certain extent due to the increase in the structural density and interaction between the water and guest molecule, whereas the decrease in the HKUST-1-S samples is mainly contributed by the water expulsion causing reduction in the overall dipole moment..

## 7.2 Imaginary part of dielectric constant ( $\epsilon''$ )

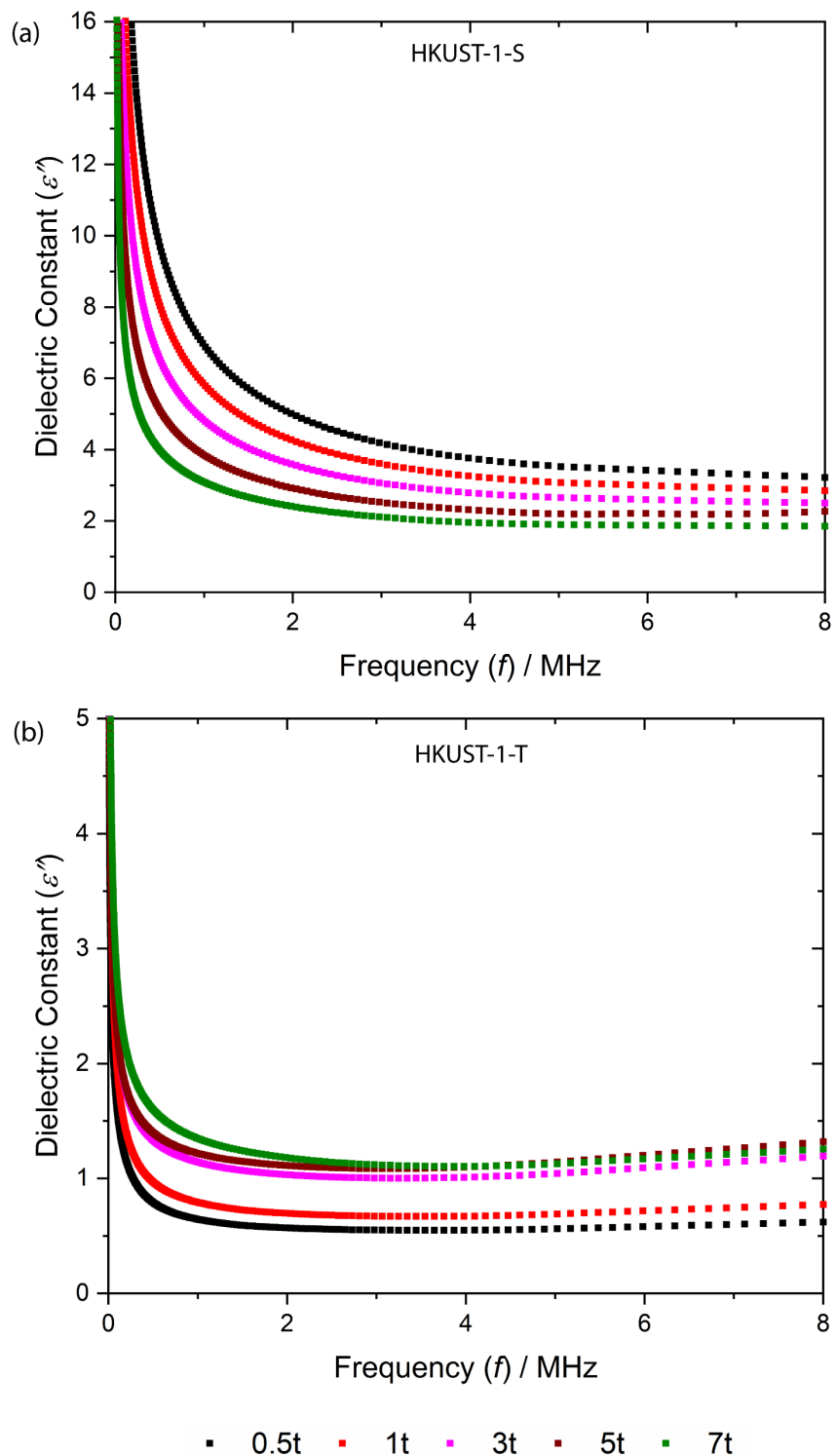


Figure S16: Imaginary part of dielectric constant of (a) HKUST-1-S and (b) HKUST-1-T pellets at ambient condition.

### 7.3 Loss Tangent ( $\tan \delta$ )

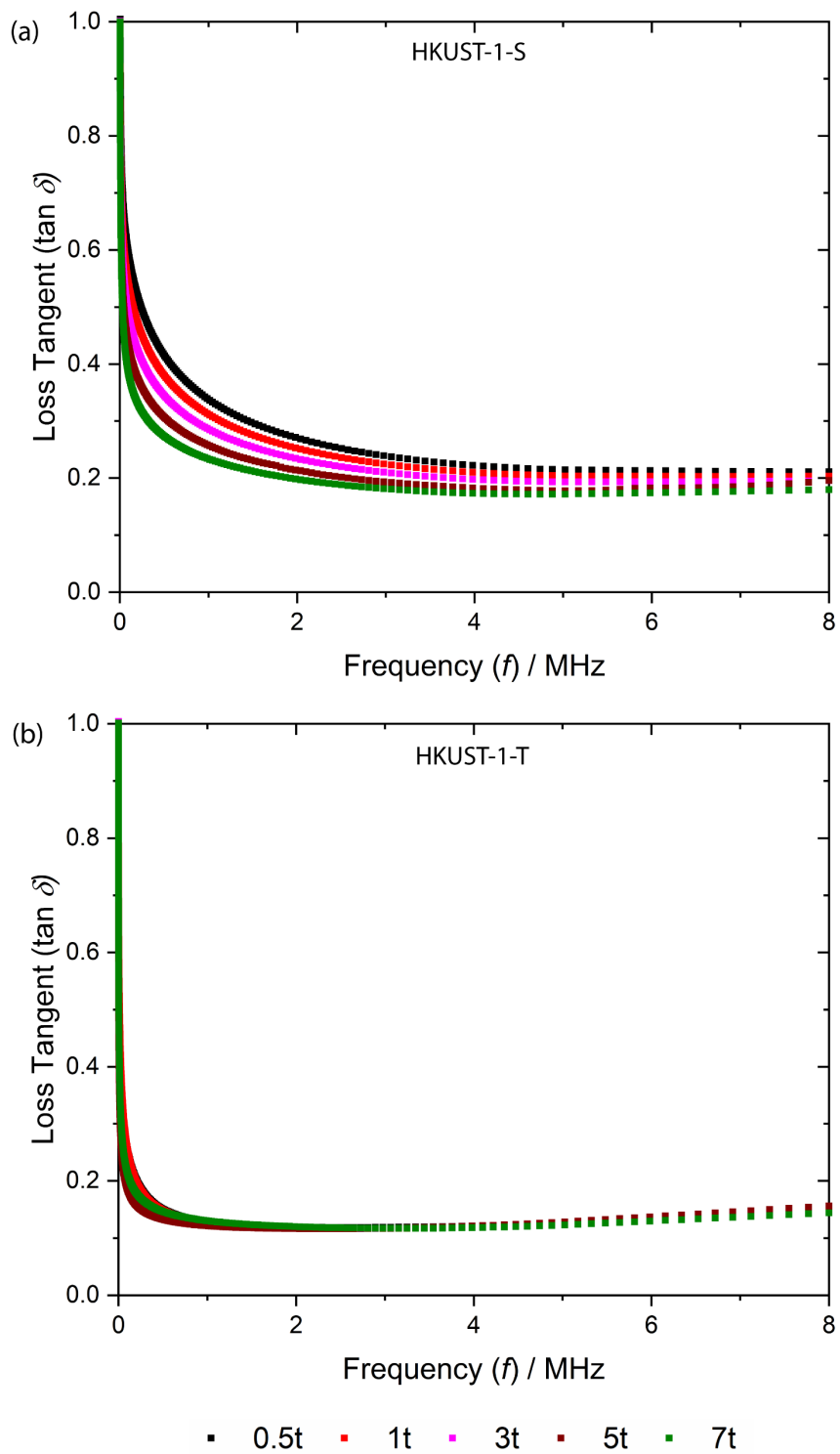
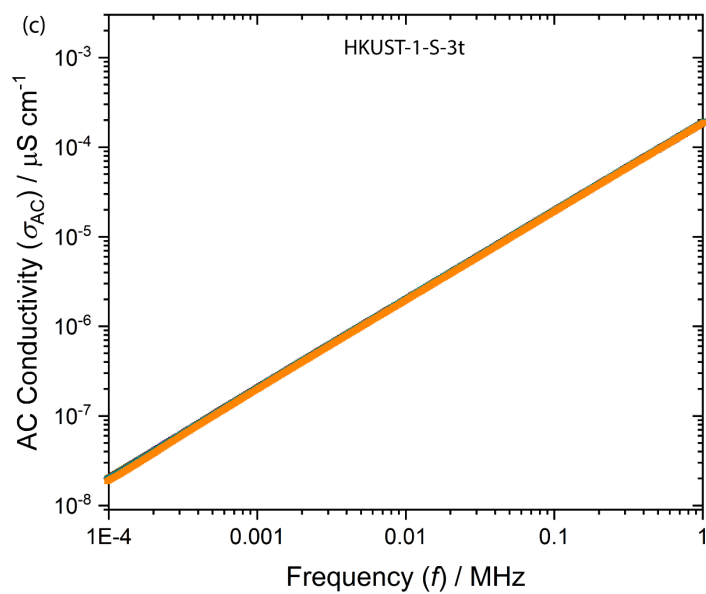
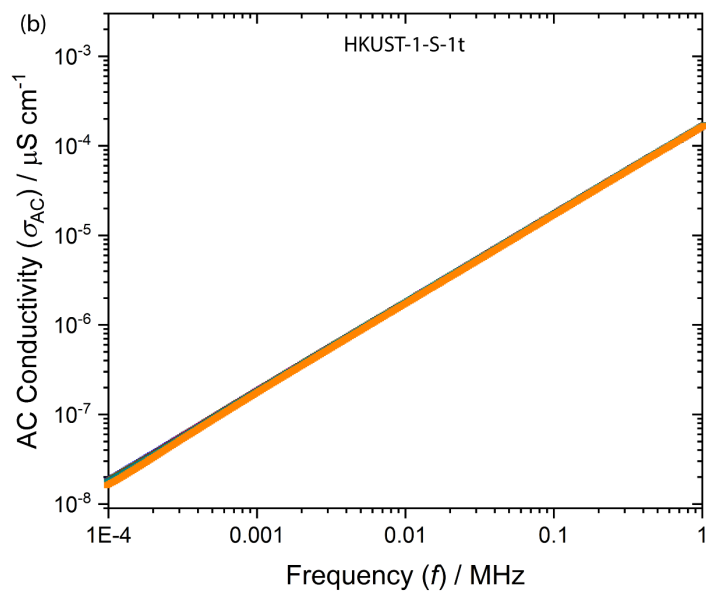
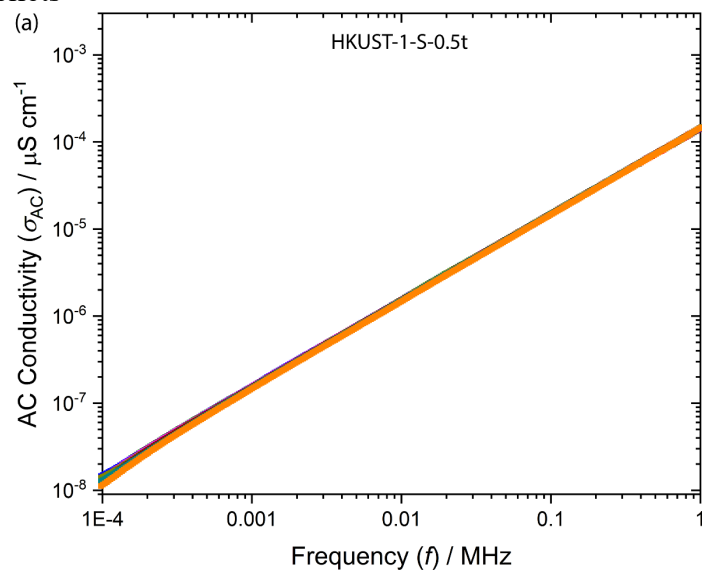


Figure S17: Dielectric loss of (a) HKUST-1-S and (b) HKUST-1-T pellets at ambient condition.

## 8 Conductivity measurements

### 8.1 AC conductivity ( $\sigma_{AC}$ )

#### 8.1.1 HKUST-1-S pellets



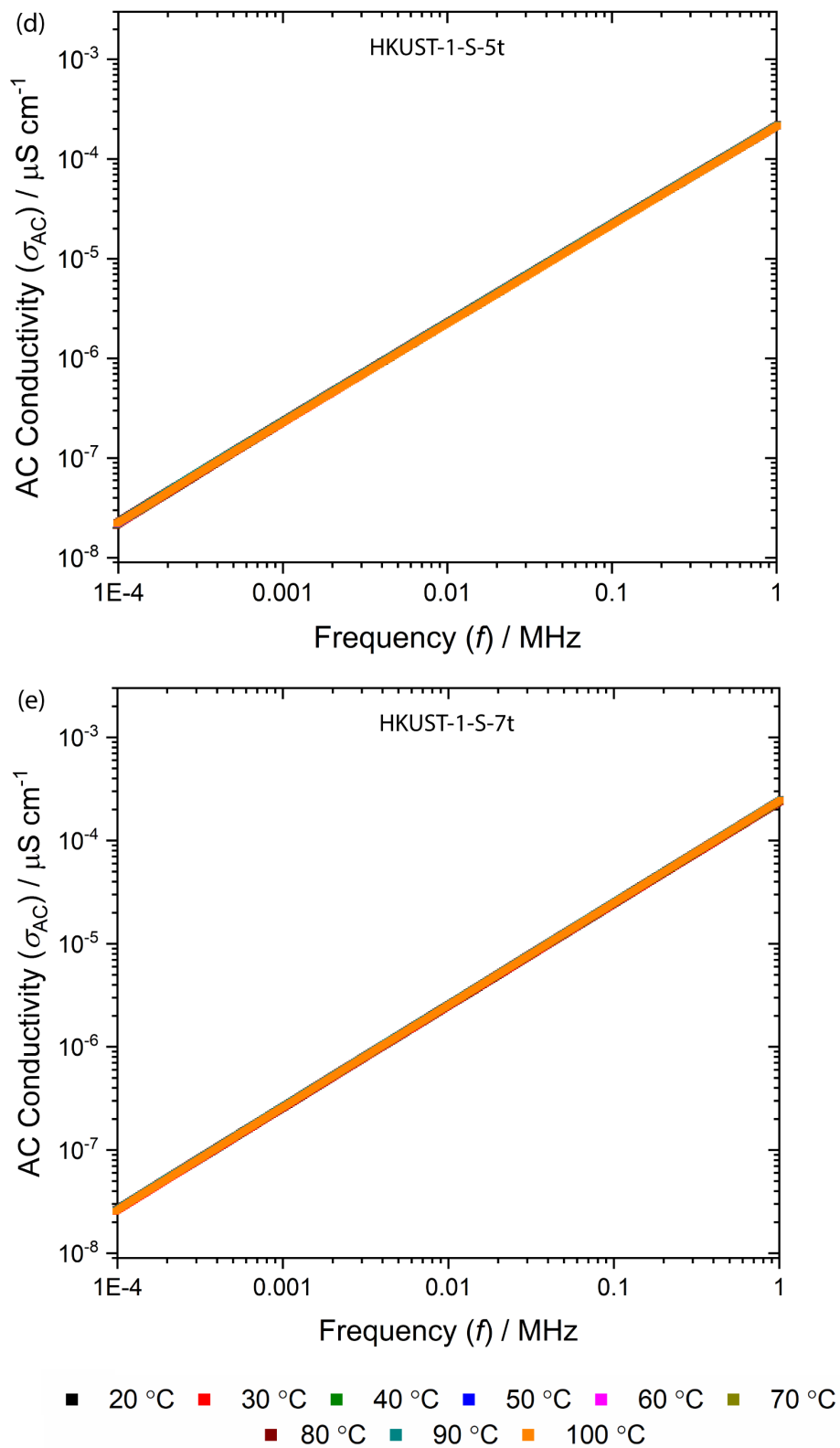
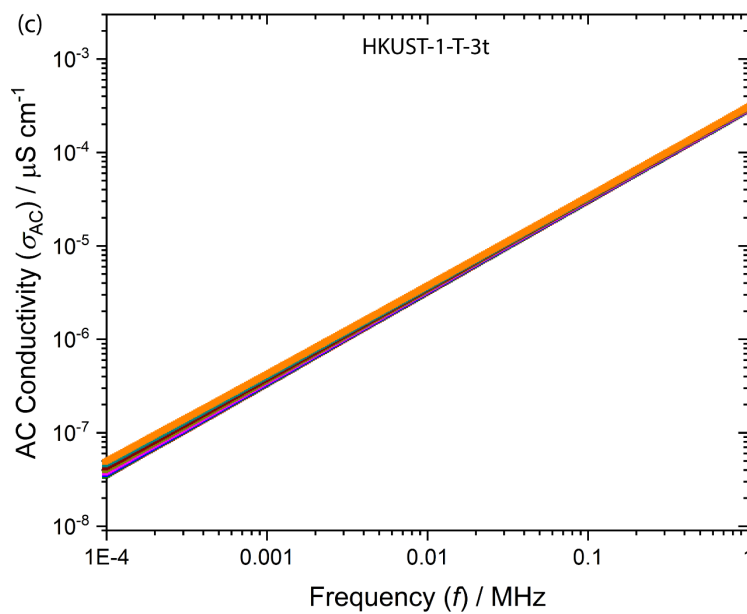
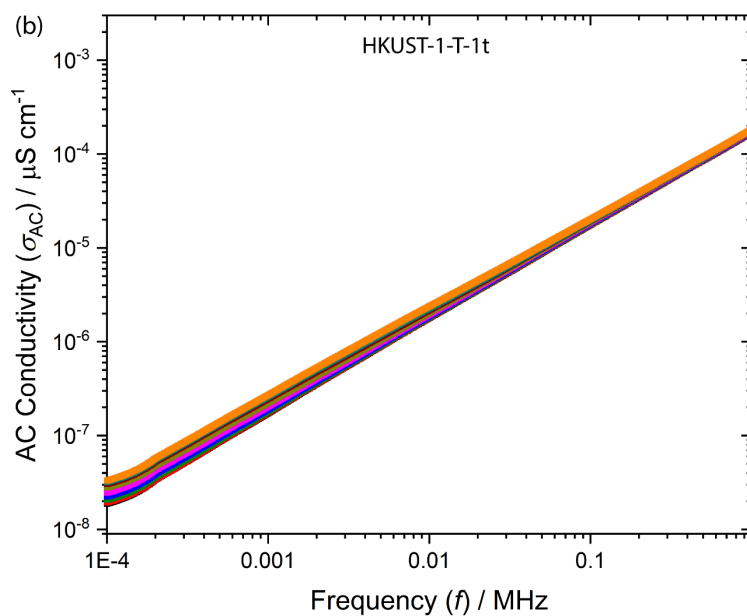
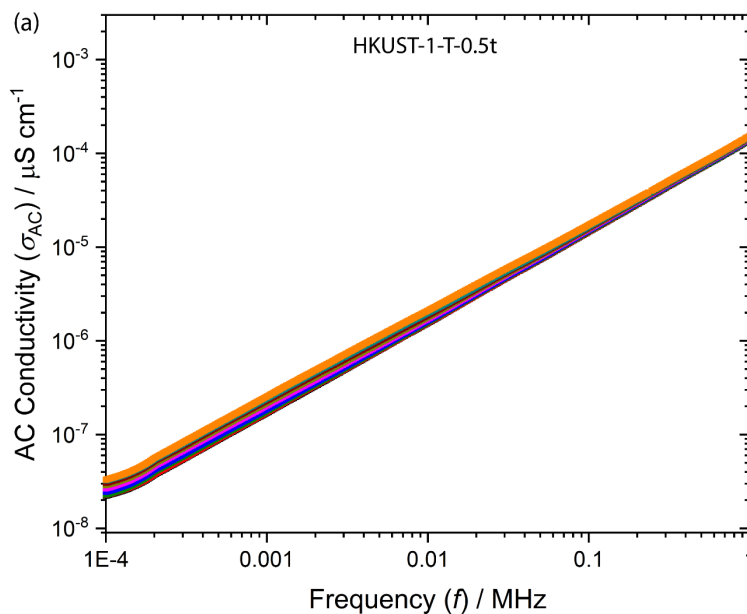


Figure S18: Temperature dependent Ac conductivity as a function of frequency for HKUST-1-S pellets prepared under a compression load of: (a) 0.5 ton, (b) 1 ton, (c) 3 ton, (d) 5 ton and (e) 7 ton, corresponding to the pressure of 36.96, 73.92, 221.76, 369.6 and 517.44 MPa, respectively.

### 8.1.2 HKUST-1-T pellets



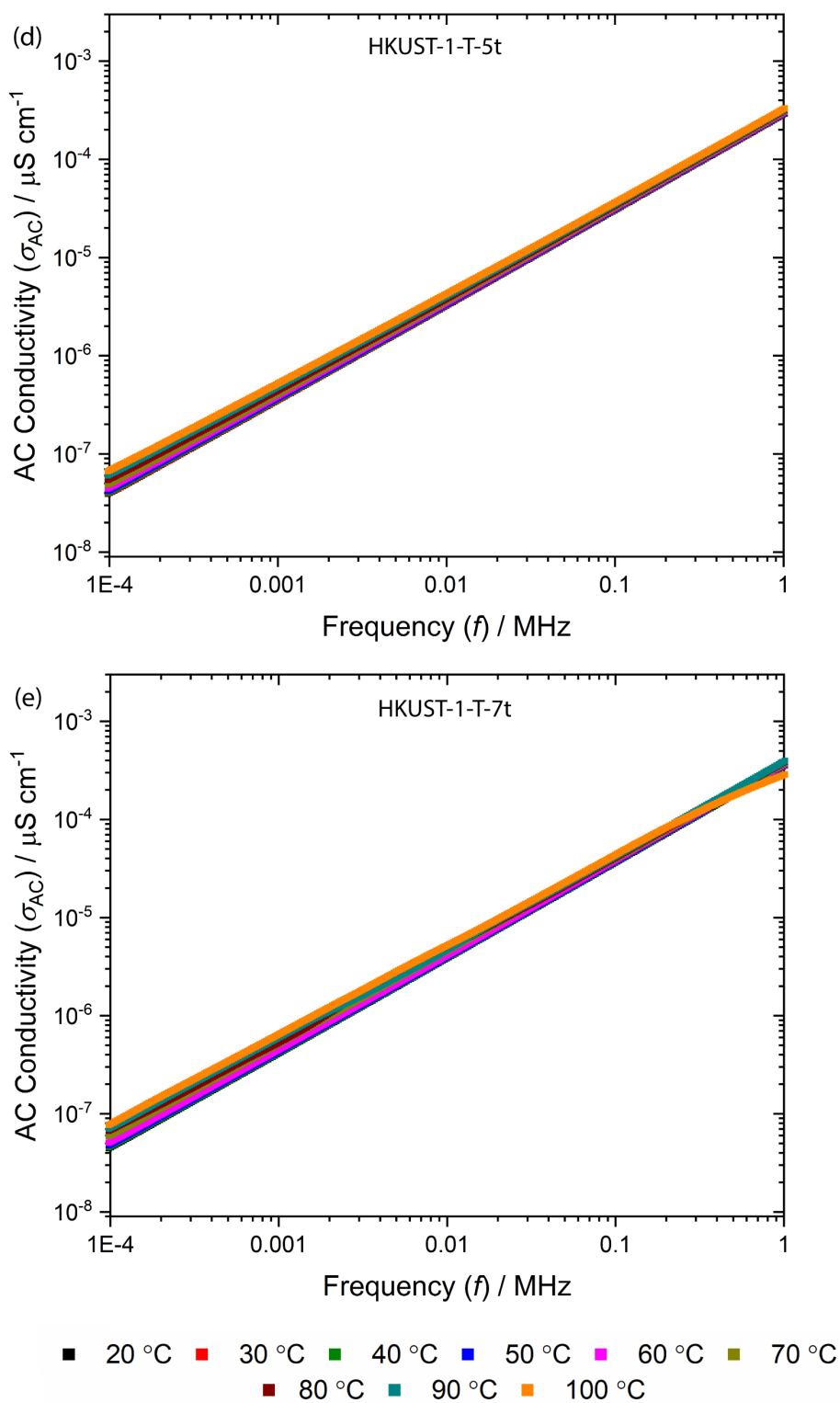
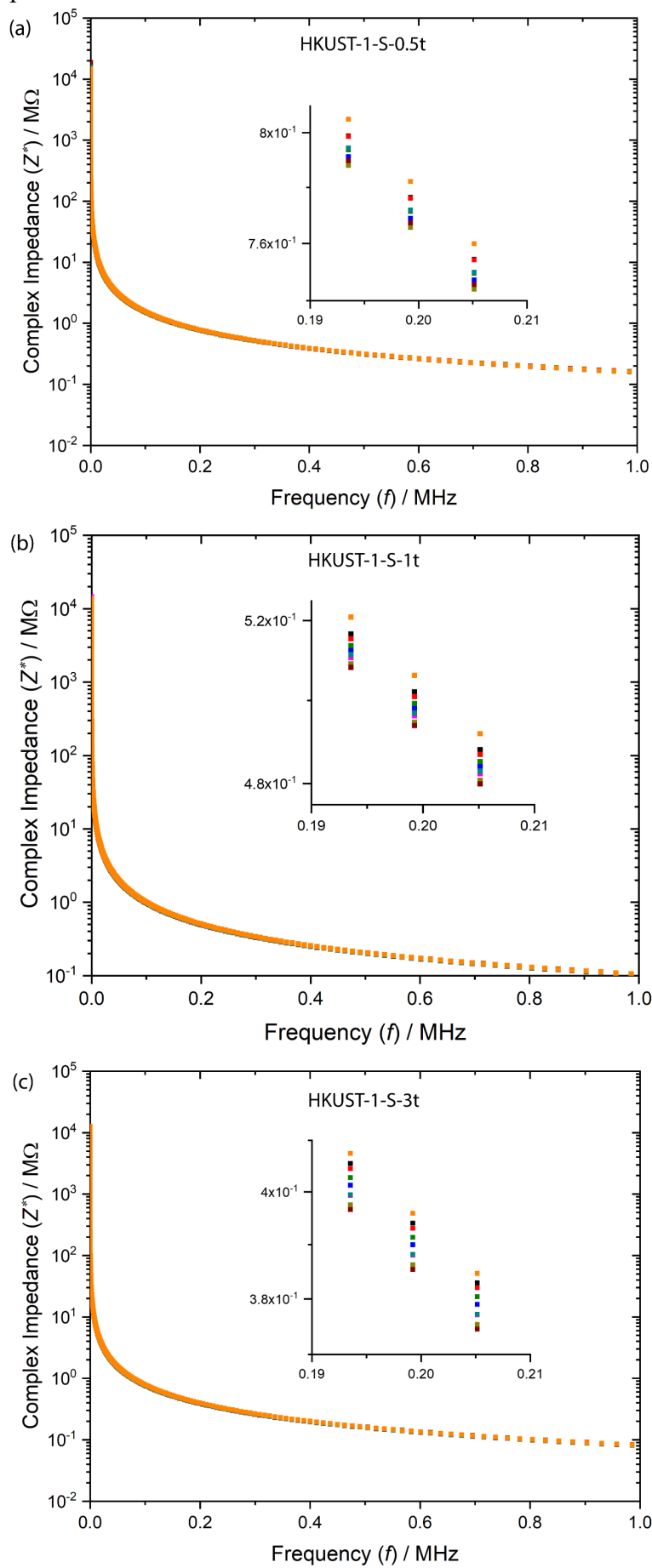


Figure S19: Temperature dependent AC conductivity as a function of frequency for HKUST-1-T pellets: (a) 0.5 ton, (b) 1 ton, (c) 3 ton, (d) 5 ton and (e) 7 ton.

## 8.2 Impedance measurements ( $Z^*$ )

### 8.2.1 HKUST-1-S pellets



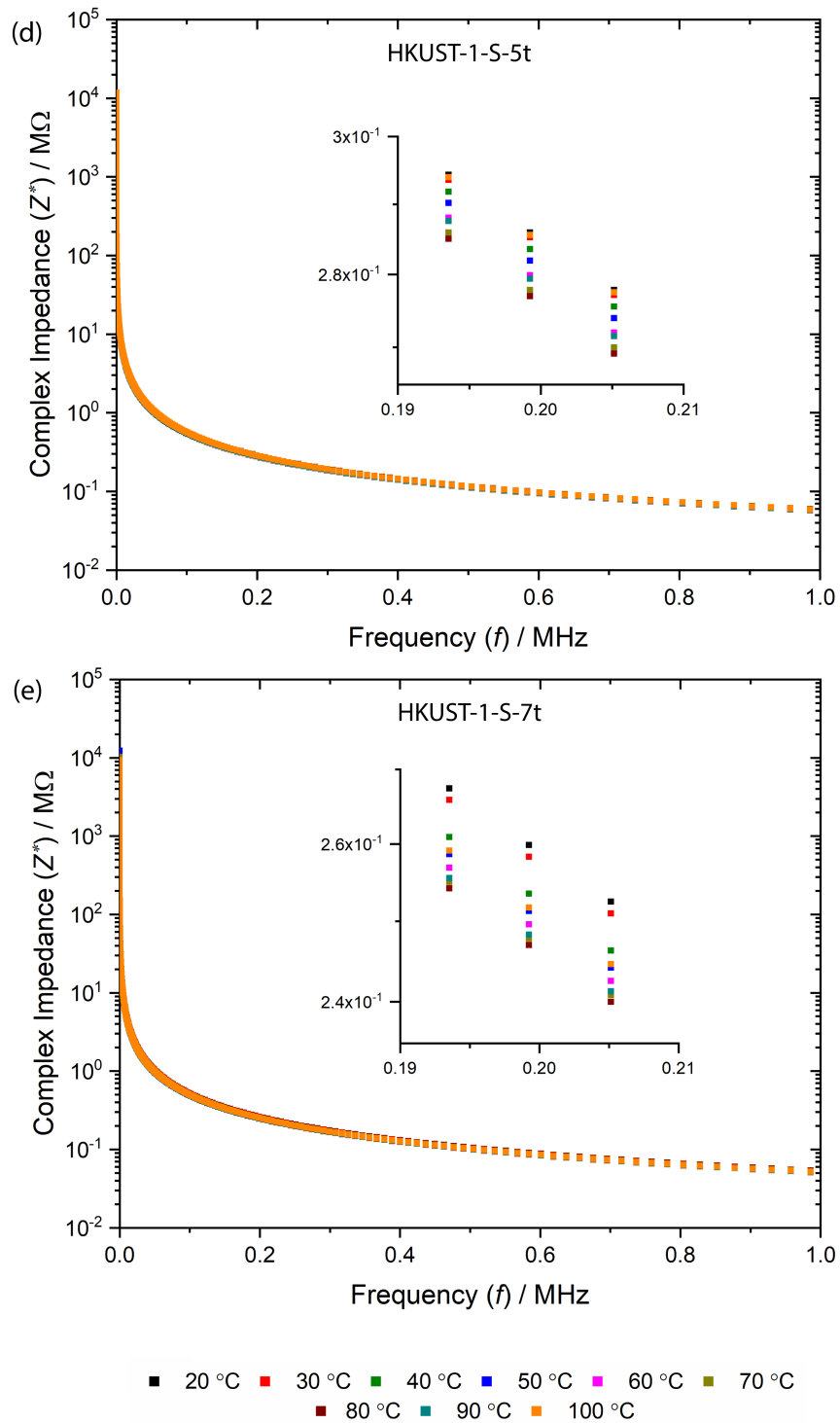
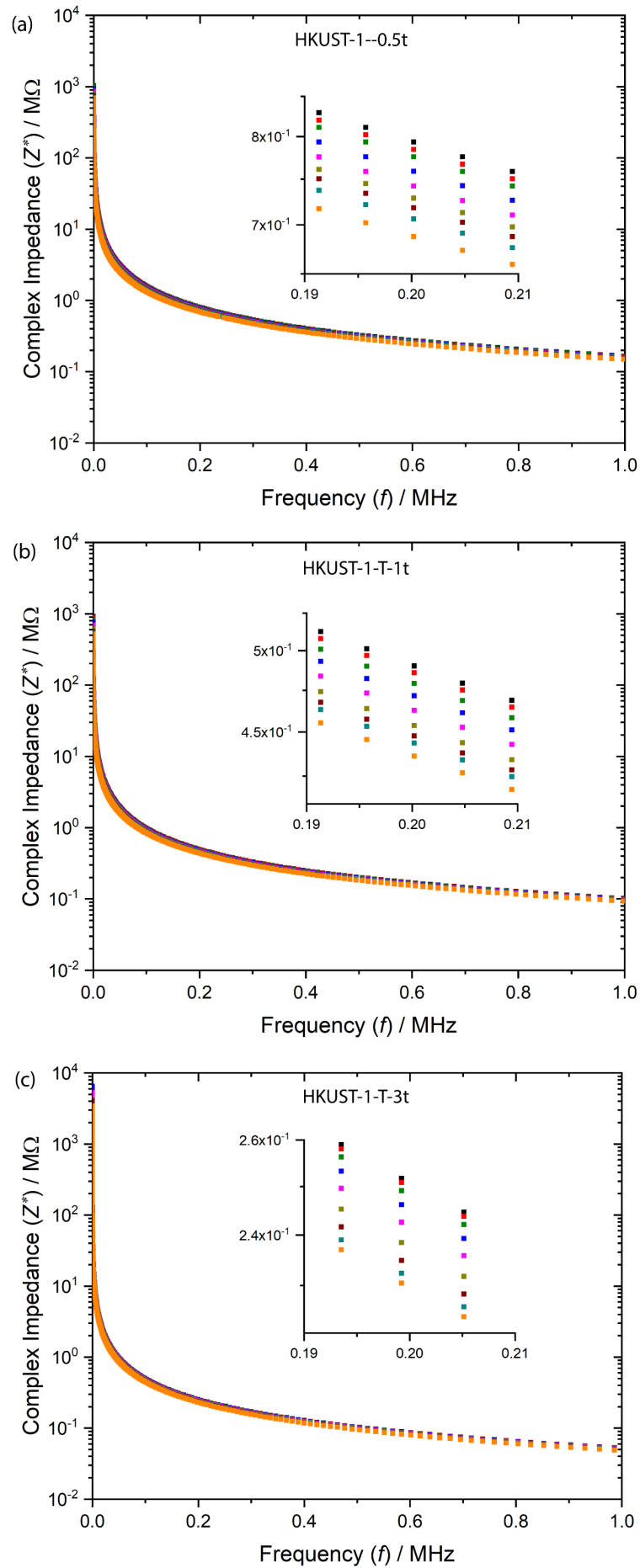


Figure S21: Temperature dependent impedance as a function of frequency for HKUST-1-S pellets prepared under a compression load of: (a) 0.5 ton, (b) 1 ton, (c) 3 ton, (d) 5 ton and (e) 7 ton, corresponding to the pressure of 36.96, 73.92, 221.76, 369.6 and 517.44 MPa, respectively.

## 8.2.2 HKUST-1-T pellets



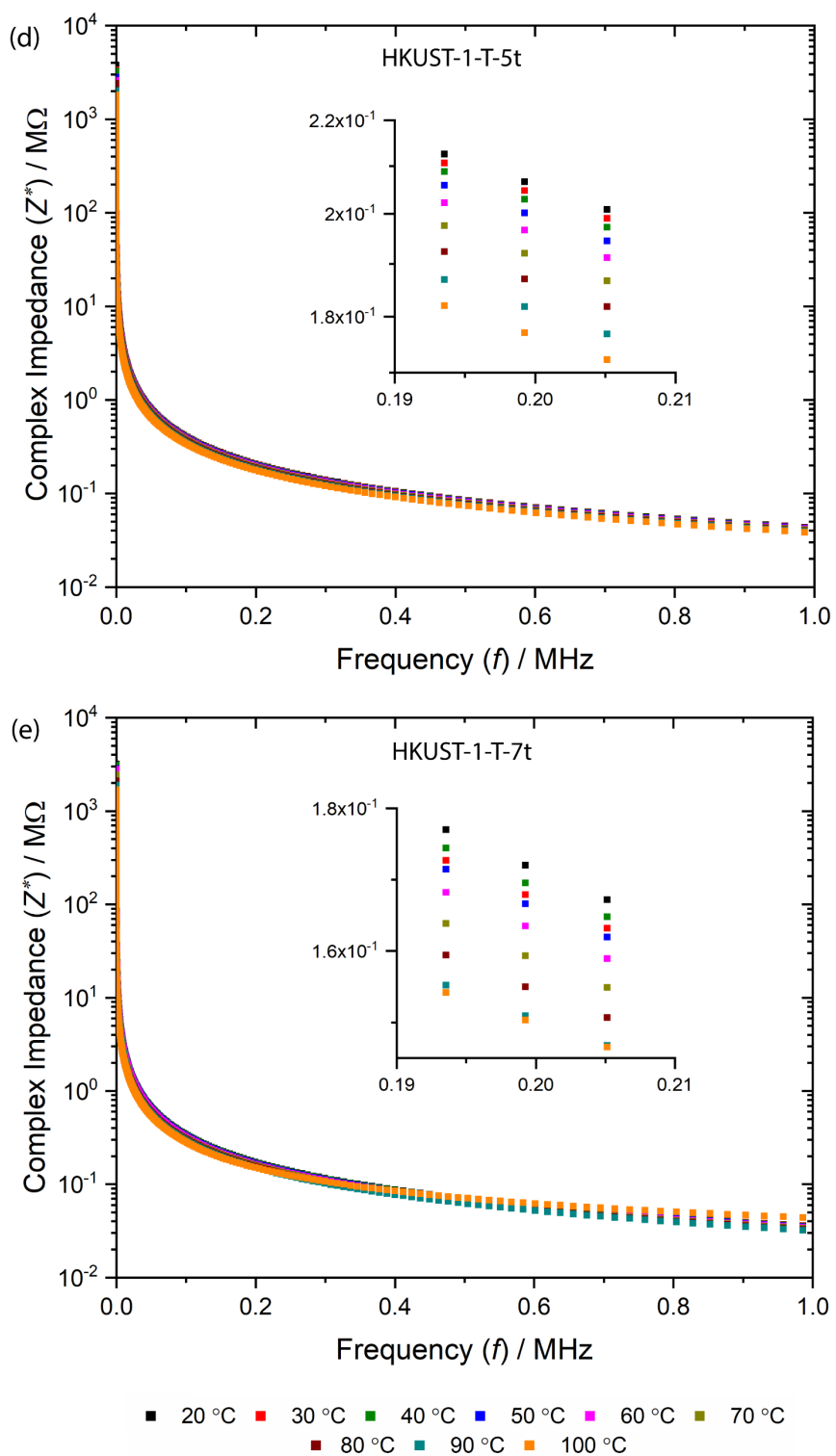


Figure S22: Temperature dependent impedance as a function of frequency for HKUST-1-T pellets: (a) 0.5 ton, (b) 1 ton, (c) 3 ton, (d) 5 ton and (e) 7 ton.

### 8.2.3 Complex impedance of pellets at ambient conditions (44% RH)

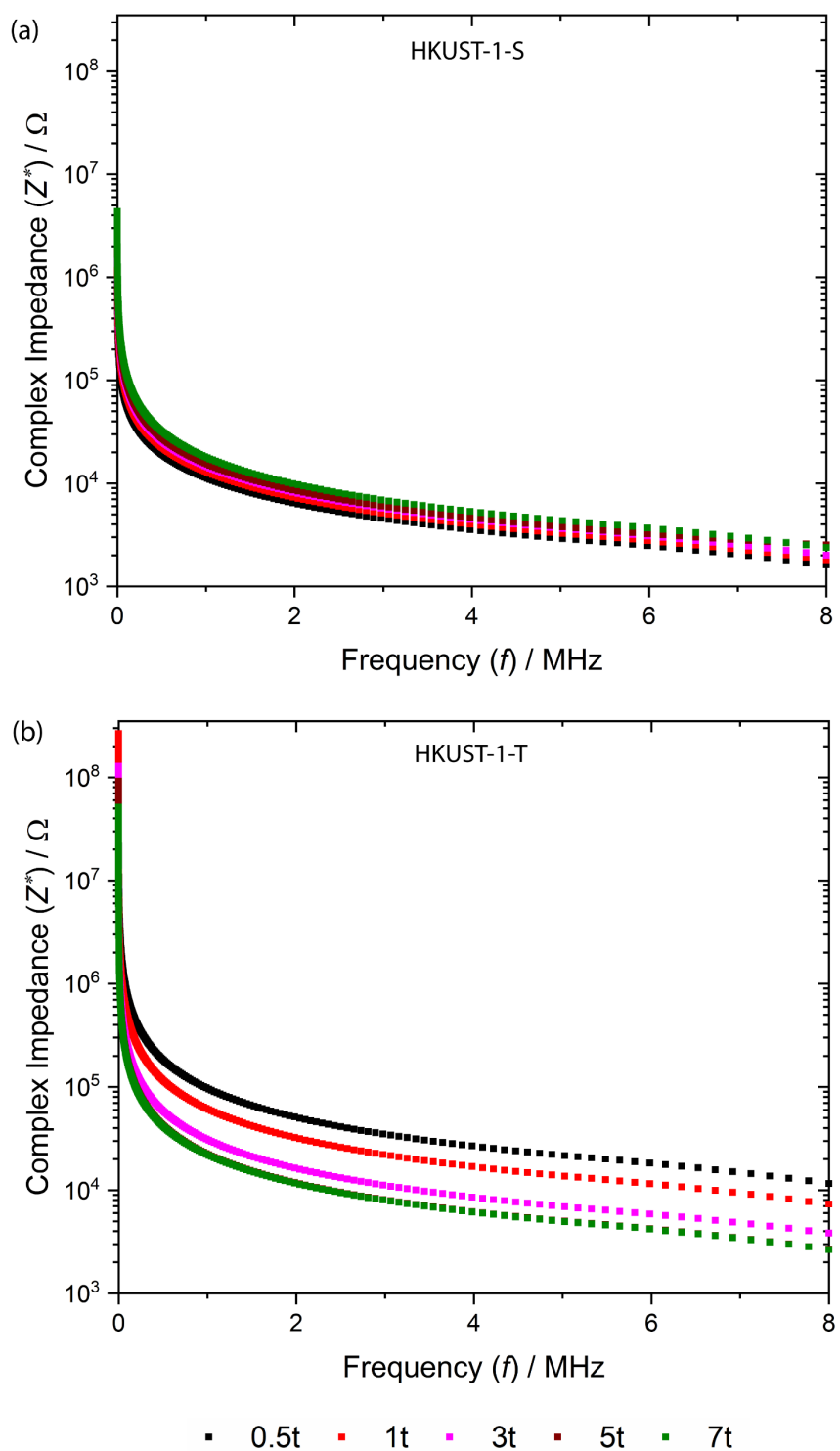
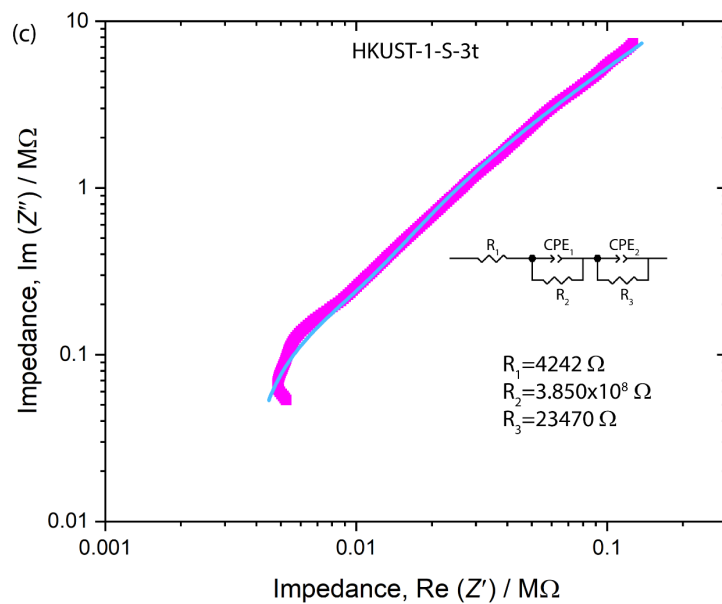
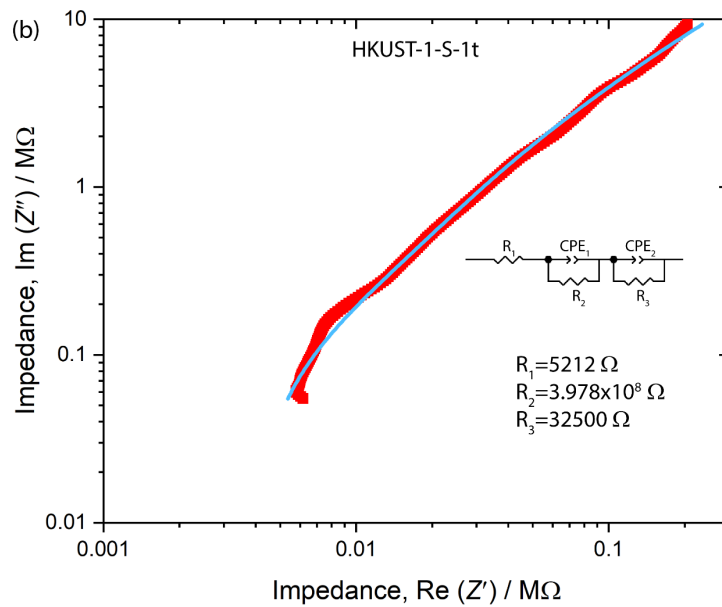
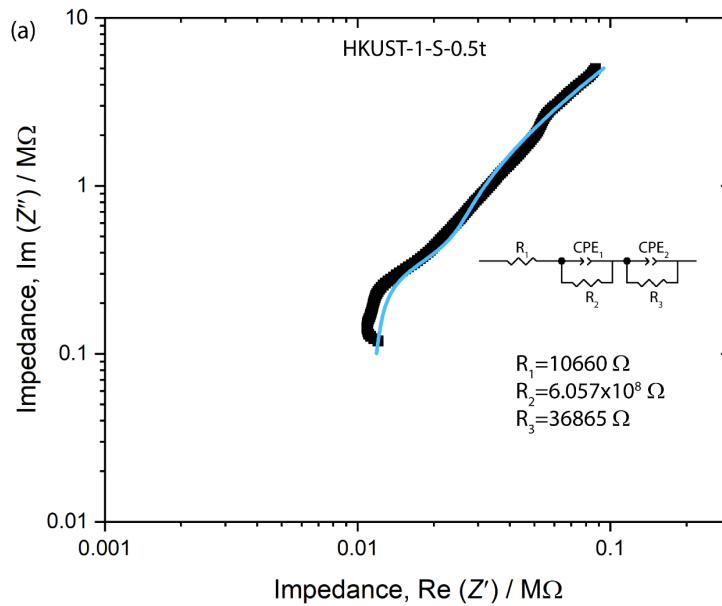


Figure 23: Plot Complex impedance with frequency for (a) HKUST-1-S and (b) HKUST-1-T at ambient condition.

## 9 Equivalent circuit data fitting of impedance plot

### 9.1 HKUST-1-S pellets



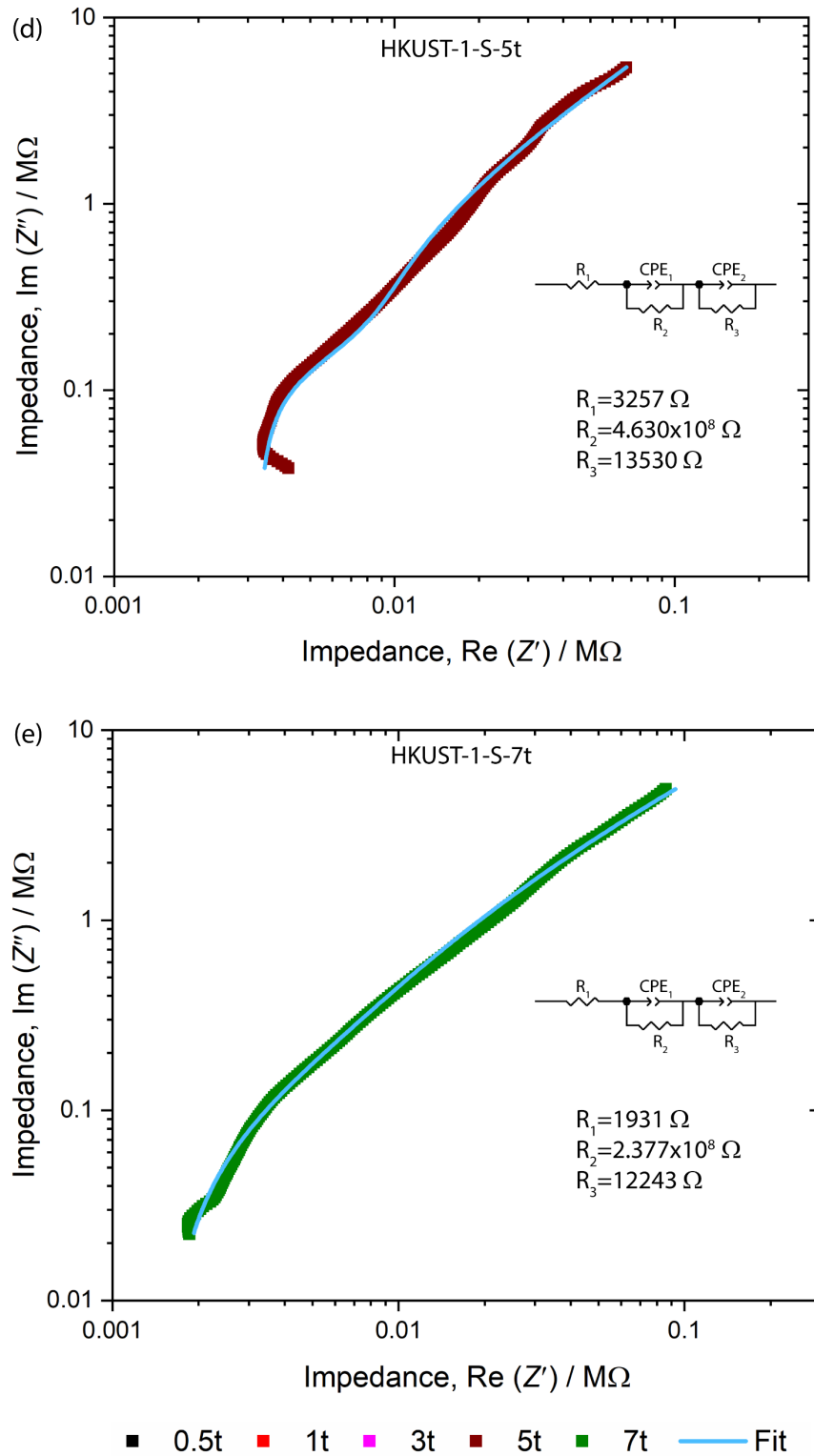
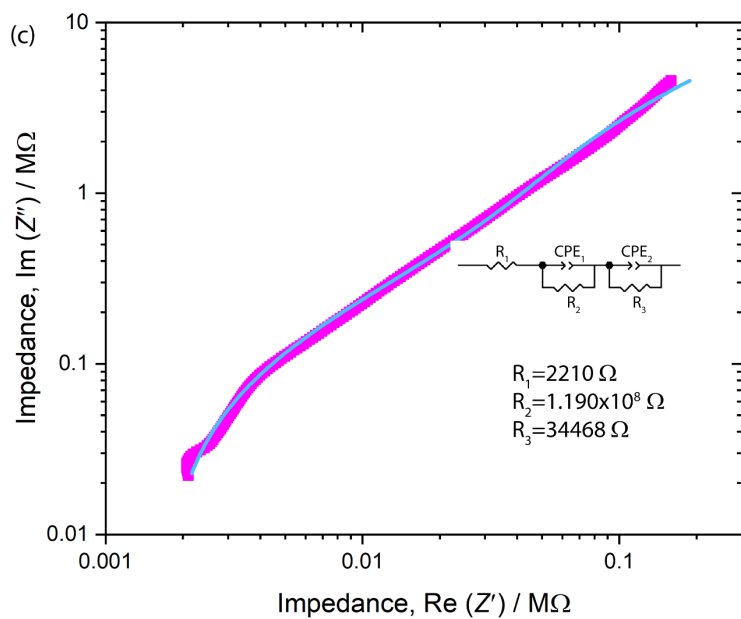
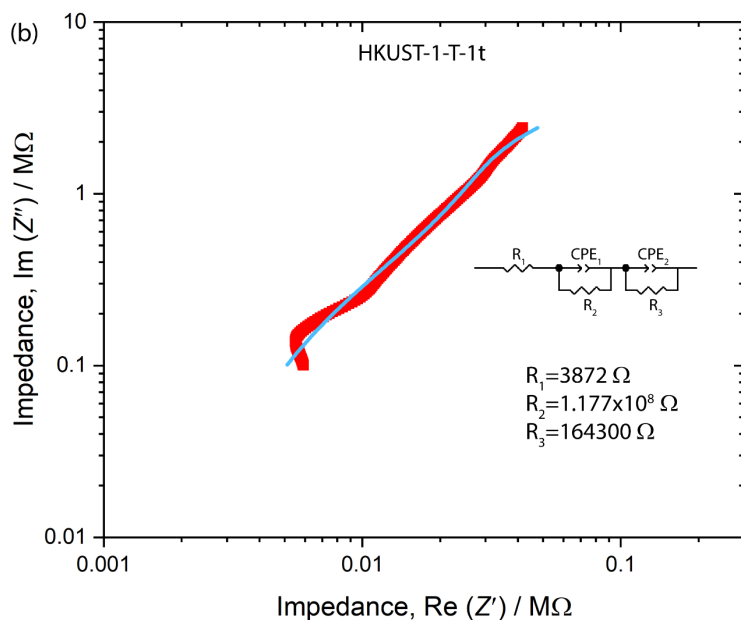
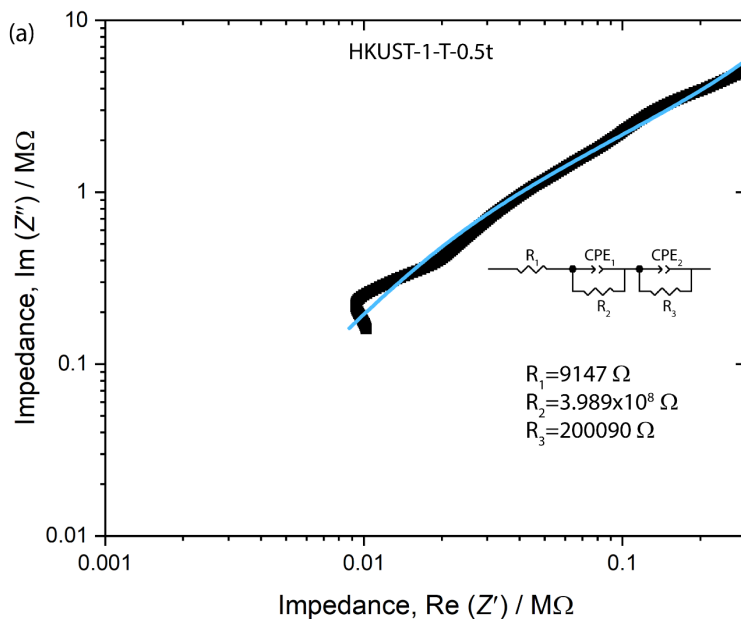


Figure 24: Impedance plot of real impedance vs imaginary impedance with the equivalent circuit curve fit at 20 °C for HKUST-1-S: (a) 0.5 ton, (b) 1 ton, (c) 3 ton, (d) 5 ton and (e) 7 ton, corresponding to the pressure of 36.96, 73.92, 221.76, 369.6 and 517.44 MPa, respectively.

9.2 HKUST-1-T



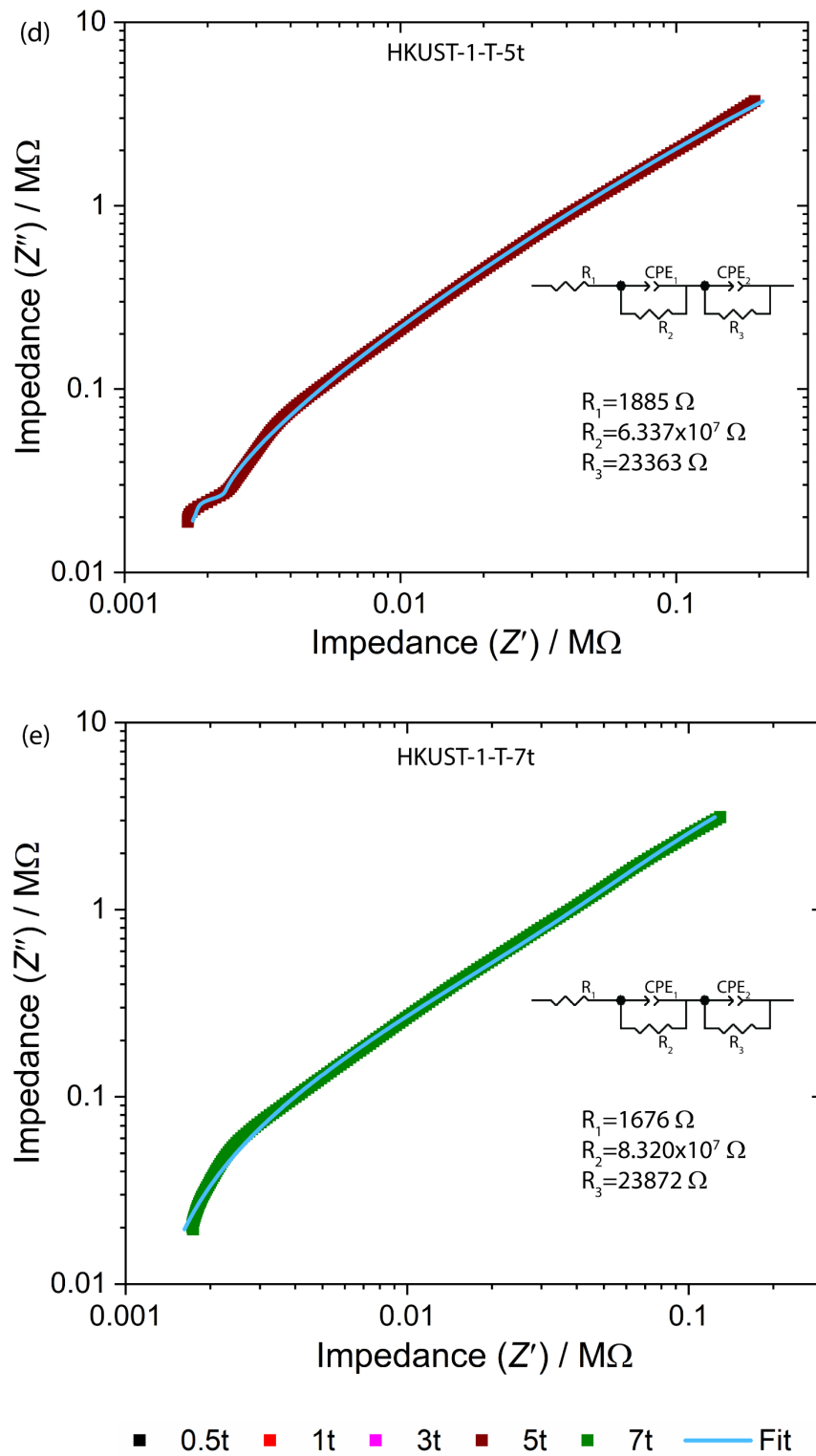


Figure 25: Impedance plot of real impedance vs imaginary impedance with the equivalent circuit at 20 °C for HKUST-1-T: (a) 0.5 ton, (b) 1 ton, (c) 3 ton, (d) 5 ton and (e) 7 ton.

Table S1: Conductivity of HKUST-1 pellets calculated by fitting the equivalent circuit in the impedance data.

Sample designation	Conductivity (S cm <sup>-1</sup> )			
	HKUST-1-S		HKUST-1-T	
	20 °C	100 °C	20 °C	100 °C
0.5t	$1.65 \times 10^{-8}$	$2.79 \times 10^{-8}$	$2.51 \times 10^{-8}$	$1.16 \times 10^{-7}$
1t	$2.51 \times 10^{-8}$	$2.23 \times 10^{-8}$	$5.63 \times 10^{-8}$	$1.39 \times 10^{-7}$
3t	$2.59 \times 10^{-8}$	$2.32 \times 10^{-8}$	$8.40 \times 10^{-8}$	$2.05 \times 10^{-7}$
5t	$2.16 \times 10^{-8}$	$2.98 \times 10^{-8}$	$1.58 \times 10^{-7}$	$4.39 \times 10^{-7}$
7t	$4.21 \times 10^{-8}$	$4.25 \times 10^{-8}$	$1.020 \times 10^{-7}$	$5.37 \times 10^{-7}$